

# Capacity Scaling of Ad Hoc Networks with Spatial Diversity

Andrew M. Hunter, *Student Member, IEEE*, Jeffrey G. Andrews, *Senior Member, IEEE*,  
and Steven P. Weber, *Member, IEEE*

**Abstract**—This paper derives the exact outage probability and transmission capacity of ad hoc wireless networks with nodes employing multiple antenna diversity techniques. The analysis enables a direct comparison of the number of simultaneous transmissions achieving a certain data rate under different diversity techniques. Preliminary results derive the outage probability and transmission capacity for a general class of signal distributions which facilitates quantifying the gain for fading or non-fading environments. The transmission capacity is then given for uniformly random networks with path loss exponent  $\alpha > 2$  in which nodes: (1) use static beamforming through  $M$  sectorized antennas for which the gain is shown to be  $\Theta(M^2)$  if the antennas are without sidelobes, but less in the event of a nonzero sidelobe level; (2) dynamic eigen-beamforming (maximal ratio transmission/combining) in which the gain is shown to be  $\Theta(M^{\frac{2}{\alpha}})$ ; (3) various transmit antenna selection and receive antenna selection combining schemes which give appreciable but rapidly diminishing gains; and (4) orthogonal space-time block coding, for which there is only a small gain due to channel hardening that increases with the number of transmit antennas, which is equivalent to the gain due to Nakagami- $m$  fading for increasing  $m$ . It is concluded that in ad hoc networks, static and dynamic beamforming perform best, selection combining performs well but with rapidly diminishing returns with added antennas, and that space-time block coding offers only marginal gains.

## I. INTRODUCTION

PRIOR work on ad hoc network capacity has focused on the limiting behavior as the network grows large. For the purpose of ascertaining the effect that multiple antennas has on the capacity of the network, the more pertinent question is how the capacity scales with the number of antennas at each node. Naturally, this scaling will differ depending on the way that the antennas are utilized. The goal of this paper is to determine which multiple-antenna techniques perform best in a given network density or similarly, which technique can support the densest network.

Multi-antenna systems (MIMO) are currently of great interest in all wireless communication systems due to their potential to combat fading, increase spectral efficiency, and potentially reduce interference. Over the past decade, many different MIMO techniques have been proposed, which can be grouped into three

broad categories: diversity-achieving, beam-steering, and spatial multiplexing. Diversity-achieving techniques increase reliability by combatting or exploiting channel variations. Beam-steering techniques increase received signal quality by focusing desired energy or attenuating undesired interference. Spatial multiplexing aggressively increases the data rate by transmitting independent data symbols across the antenna array. In this paper we focus on the first two types of techniques, which do not increase the number of independent datastreams and hence are easier to fairly compare. We also expect that these more conservative techniques are likely to be more relevant than spatial multiplexing in a dense (i.e. interference-limited) ad hoc network, based on MIMO research in low-SNR links [1], [2]. This paper develops a framework for comparing the utility of the diversity-providing and beam-steering MIMO techniques, with the goal of providing insight on how to use multiple antennas in ad hoc networks.

### A. Background and Related Work

Recent advances in characterizing network capacity were sparked by [3] with its notion of transport capacity and a number of works have followed in the same vein including [4], [5], [6], [7]. These studies focus on the behavior of end-to-end network capacity in the limit as the number of nodes grows large under a variety of models of node interaction and fading conditions. These confirm the basic intuition from [3] that transmissions require “area” in which to take place and so per node end-to-end throughput decays as  $\Theta(\frac{1}{\sqrt{n}})$  for  $n$  nodes in the network. A fundamental change occurs with significant mobility as [8] and [9] show since optimal routing can take on new forms to tradeoff throughput and delay.

The studies particularly of network transport capacity have yielded a few key insights. Most notable is that under practical limits on delay and cooperation and under a technological model of signal reception, network capacity decays as the network grows large. This stems from the fact that transmissions require “area” in which to take place. Furthermore, there are constraints on the area taken up by each transmission due to the need both to connect the network and to maximize its spatial reuse [10], [3]. Yet, a practical perspective on these facts is that, given specific system characteristics and desired performance, a network size or density exists at which the performance goals are ultimately insupportable. That is, a primary influence on performance, as viewed from each node, is the density of transmitters contending for that channel.

An alternative characterization of ad hoc network capacity was developed in [11] which defined rate regions for given network

This work was supported by National Instruments and by the NSF under grant no. 0635003 (Weber), no. 0634979 (Andrews), and the DARPA IT-MANET program, Grant W911NF-07-1-0028.

A. M. Hunter and J. G. Andrews are with the Wireless Networking and Communications Group (WNCG) of the Electrical and Computer Engineering Department, The University of Texas at Austin, Austin, TX, 78712-0240 USA (email: {hunter, jandrews}@ece.utexas.edu).

S. P. Weber is with the Department of Electrical and Computer Engineering, Drexel University, Philadelphia, PA 19104-2875 USA (email: sweber@ece.drexel.edu).

configurations and traffic needs. This was extended to the MIMO case in [12] and the notion of “capacity region” was extended in several ways. While this is a versatile approach for capturing network interactions, it is also prohibitively computationally intensive for analyzing large networks. It also focuses on large network optimization problems that would be difficult to solve in a distributed system at present. A randomly connected network model was studied in [13] which can be valuable for analyzing dense sensor networks when fading is the dominant propagation phenomenon. However, it deliberately ignores topology induced by distance-dependent attenuation and so its utility is limited for larger scale mesh networking.

Hence, in the design of a wireless network it is natural to approach the problem of what network density is acceptable given data rate, SINR, and outage requirements and given the physical, MAC, or network layer resources and techniques available. Furthermore, a straightforward way to evaluate a physical layer technique under given per node service requirements is to determine the maximum allowable density of concurrent transmissions, or the *optimal contention density*, for which each node’s requirements are still met. This leads naturally to the transmission capacity metric which is defined in [14] to be the maximum allowable spatial density of successful transmissions multiplied by their data rate given an outage constraint. For an outage constraint  $\epsilon$  and a transmission data rate  $b$  in bits/Hz or per channel use, the transmission capacity is given by  $c_\epsilon = b(1 - \epsilon)\lambda_\epsilon$  for the optimal contention density  $\lambda_\epsilon$ . The transmission capacity is then the area spectral efficiency resulting from the optimal contention density.

The transmission capacity framework provides a way both to relate properties of the physical layer to network performance as well as a means to compare various techniques. Previous transmission capacity results include Weber, *et al.* [14], who derived bounds on optimal contention densities for networks using single-antenna CDMA systems in a simple path loss only model, giving a clear relationship between the spreading gain and the transmission capacity. They also include Baccelli, *et al.* [15], who derived the maximum transmission capacity (though not under this name) for single-antenna systems with exponentially distributed power factors (which is equivalent to a Rayleigh fading channel model in addition to path loss attenuation) *en route* to a protocol analysis.

These results rely on properties of spatial point process which were pioneered in the analysis of wireless networks by [16] and [17]. Chan and Hanly [18] then related the outage probability to characteristics of spatial Poisson traffic in the cellular CDMA context. Recently, Haenggi, *et al.* in [19], [20], and [21] emphasized the importance of network topology by characterizing some of the distinctions in throughput, interference, and outage in regular as well as uniform and clustered stochastic networks. Srinivasa and Haenggi [22] extended the end-to-end reliability analysis of “erristors” developed in [19] to MIMO selection combining.

Much research in the past decade has been devoted to enumerating and evaluating the benefits of MIMO in point-to-point links both for increased diversity and increased capacity (see [23] and [24] and its references). Several papers, including [25], [26], [27], incorporated the effects of cochannel interference. These analyzed beamforming MIMO systems with equal power

co-channel interferers in a variety of fading environments using techniques such as maximal ratio transmission (MRT), maximal ratio combining (MRC), and also optimal combining. However, these studies lack a clear link between point-to-point throughput and network performance gains and do not provide simple means of considering random topologies.

Furthermore, it is unclear which MIMO technologies yield the highest gains in large random networks. For example, [28] based on a game-theoretic analysis shows that capacity is maximized for mutually interfering sources when each sends only one datastream, while [29] and [30] suggest capacity is improved through spatially multiplexing potentially multiple transmissions; however, [29] again focuses on asymptotics in the number of nodes and the results of [30] are obscured by the mobility/delay issue. Furthermore, [1] and [22] show that the reliability of MIMO is highly dependent on the SNR. A recent notable result in [29] gives a network spectral efficiency bound for MIMO ad hoc networks analyzing the throughput of a set of transmitter-receiver pairs. The implication is again that throughput decays with increasing network size unless a large degree of interfering channel information and coordination are available. The study also shows the optimality of beamforming without elaborate channel state information. Based on limited numerical work [12] indicates that many MIMO techniques perform similarly in networks as in point-to-point links. However, some specific counterexamples will be established here showing the presence of interference alters the relative gains of diversity techniques on network capacity.

## B. Contributions

This paper analyzes networks with single-datastream MIMO diversity techniques including beamforming, antenna sectorization, space-time block coding, and selection combining in Rayleigh fading. The gains in transmission capacity of each are shown, especially as a function of the number of antennas, and they are compared. Results are also given for Nakagami- $m$  fading for integer  $m$  to compare methods in line-of-sight versus non-line-of-sight propagation environments and to assist in interpreting channel hardening gains. While spatial multiplexing techniques are omitted, they are left as future work though some of the results developed here will also be applicable to spatial multiplexing systems. Since diversity techniques are robust in noise-limited environments and generally reasonable to implement, they constitute an important subset of the primary MIMO techniques. Also, as indicated in [28] some game-theoretic analysis indicates optimality of single stream techniques.

For random wireless networks using the above techniques in block fading channels with path loss, this paper determines transmission capacity, the scaling of the optimal contention density with the number of antennas, and outage probabilities as a function of network parameters. In addition to exact results, the paper derives the following relations between the optimal contention density and the number of antennas for  $M_t$  and  $M_r$  are the number of transmit and receive antennas, respectively, and  $\alpha > 2$  is the path loss exponent:

- 1) Ideal Sectorized Antennas:  $\lambda_\epsilon = \Theta(M_t M_r)$

2) Sectorized Antennas with sidelobe level  $\gamma \in [0, 1]$ :

$$\lambda_\epsilon = \Theta \left[ \left( \frac{M}{1+\gamma^{\frac{2}{\alpha}}(M-1)} \right)^2 \right] \text{ for } M = M_t = M_r$$

3) Maximal Ratio Combining:  $\lambda_\epsilon = \Theta(M_r^{\frac{2}{\alpha}})$

4) Maximal Ratio Transmission and Combining:  
 $\lambda_\epsilon = \Theta((M_t M_r)^{\frac{2}{\alpha}})$ ,  $\lambda_\epsilon = \Omega(\max\{M_t, M_r\}^{\frac{2}{\alpha}})$

5) Orthogonal Space-Time Block Coding:  $\lambda_\epsilon = \Omega(M_r^{\frac{2}{\alpha}})$ .

These relations demonstrate that beamforming yields the most network gains among diversity techniques while space-time block coding yields little, especially for more antennas than two, and can even be inferior to SISO systems. The results also highlight the advantages of achieving diversity at the receiver.

The remainder of the paper is organized as follows: Section II presents the network model and derives properties for Poisson shot noise functionals applicable to large class of MIMO techniques. Section III discusses the optimal contention density for single antenna systems in Nakagami- $m$  fading. The optimal contention density for networks of nodes with multiple sectorized antennas is derived in Section IV. Section V derives the outage probabilities and optimal contention densities for receive MRC systems and Section V-B does the same for MIMO MRT/MRC systems. Networks using orthogonal space-time block codes (OS-TBCs) are analyzed in Section VI. Section VII gives transmission capacity results for selection combining in ad hoc networks. Section VIII offers some discussion of the utility of MIMO in ad hoc networks and Section IX concludes.

## II. THE NETWORK MODEL AND ANALYTICAL METHODS

### A. The Model

This section defines the network model and presents some results on Laplace functionals of Poisson shot noise processes which will be used in later sections. In order to focus on the physical layer, consider a wireless network operating a random access protocol in the style of slotted ALOHA without power control. As discussed in [14], this model includes the collision behavior of practical distributed systems while neither addressing nor precluding the issue of routing. It also provides a way to give a clear relationship between the network throughput and the number of antennas employed for each technique. Let the distribution of transmitting nodes in the network be a stationary marked Poisson point process with intensity  $\lambda$  in  $\mathbb{R}^2$ ; the process is denoted by  $\Phi$ . To analyze the performance of a random access wireless network, consider a typical receiver located at the origin. As a result of Palm probabilities of a Poisson process, conditioning on the event of a node lying at the origin does not affect the statistics of the rest of the process (see [31], ch. 2). Moreover, due to stationarity of the Poisson process, the statistics of signal reception at this receiver are identical to the statistics seen by any receiver.

To model propagation through the wireless channel, let signals be subject to path loss attenuation model  $|d|^{-\alpha}$  for a distance  $d$  with exponent  $\alpha > 2$  as well as small scale fading for either a Rayleigh or Nakagami- $m$  fading distribution with unit mean. Also, let all nodes transmit with the same power  $\rho$ . For such a channel, the typical receiver obtains desired signal power

$\rho S_0 R^{-\alpha}$  for some fixed transmitter-receiver separation distance  $R$ , and with a fading power factor  $S_0$  on the signal from its intended transmitter, labeled 0. The interfering nodes, numbered 1, 2, 3, ... constitute the marked process  $\Phi = \{(X_i, S_i)\}$ , with  $X_i$  denoting the location of the  $i$ th transmitting node, and with marks  $S_i$  that denote fading factors on the power transmitted from the  $i$ th node and then received by the typical receiver. Thus the receiver receives interference power  $\rho S_i |X_i|^{-\alpha}$  from the  $i$ th interfering node. For single-antenna narrowband systems in Rayleigh fading channels, for example, the power factors  $S_0$  and  $S_i$  are distributed exponentially with unit mean so that the mean interfering power is governed by transmit power and path loss.

Successful transmission occurs if the inequality

$$\frac{\rho S_0 R^{-\alpha}}{\rho I_\Phi + N_0} \geq \beta \quad (1)$$

is satisfied for some target SINR  $\beta$ , aggregate co-channel interference  $\rho I_\Phi$ , and thermal noise  $N_0$ . The aggregate interference is a Poisson shot noise process (scaled by  $\rho$ ), which is a sum over the marked point process:

$$I_\Phi = \sum_{X_i \in \Phi} S_i |X_i|^{-\alpha} \quad (2)$$

with  $|X_i|$  denoting the distance of  $X_i$  from the origin. From here on, it will be assumed that the network is interference limited, with  $\rho, I_\Phi \gg N_0$  so that thermal noise is negligible, and normalized by setting  $\rho = 1$ . Following [15], the probability of successful transmission for a typical receiver in a uniformly random network is:

$$\begin{aligned} \mathbf{P}(SIR \geq \beta) &= \mathbf{P}\left(\frac{\rho S_0 R^{-\alpha}}{\rho I_\Phi} \geq \beta\right) \\ &= \mathbf{P}(S_0 \geq \beta R^\alpha I_\Phi) \\ &= \int_0^\infty \mathbf{P}(S_0 \geq s \beta R^\alpha) f_{I_\Phi}(s) ds \\ &= \int_0^\infty F_{S_0}^c(s \beta R^\alpha) f_{I_\Phi}(s) ds \end{aligned} \quad (3)$$

where the third step is reached by conditioning on  $s$  and  $F^c(\cdot)$  denotes a complementary cumulative distribution function (CCDF). In the SISO case, the received signal power is exponentially distributed with  $F_{S_0}^c(s \beta R^\alpha) = e^{-s \beta R^\alpha}$  so that

$$\mathbf{P}(SIR \geq \beta) = \int_0^\infty e^{-s \beta R^\alpha} f_{I_\Phi}(s) ds. \quad (4)$$

This is now a Laplace transform of the PDF of  $I_\Phi$  which gives:

$$\mathbf{P}(SIR \geq \beta) = \mathcal{L}_{I_\Phi}(\beta R^\alpha). \quad (5)$$

The Laplace transform for a general Poisson shot noise process in  $\mathbb{R}^2$  with independent, identically distributed (i.i.d.) marks  $S_i$  is given by [32]

$$\mathcal{L}_{I_\Phi}(\zeta) = \exp \left\{ -\lambda \int_{\mathbb{R}^2} 1 - E \left[ e^{-\zeta S |x|^{-\alpha}} \right] dx \right\} \quad (6)$$

where the expectation, denoted by  $E[\cdot]$ , is over  $S$  which has the same distribution as any  $S_i$ . Note that we are using the simplified attenuation function  $|d|^{-\alpha}$ . While this model is inaccurate in the near field, most notably because it explodes at the origin, for

systems operating primarily in the far field (e.g.,  $R$  is many carrier wavelengths), this inaccuracy has negligible effect for the purpose of calculating outage probabilities. One can modify the path loss function to  $\frac{1}{1+|d|^\alpha}$ , for example, as mentioned in [15] and perform the same analysis. The result is that for  $R$  well in the far field, this modification leads to the same transmission capacity conclusions though with more cumbersome analysis.

For Rayleigh fading channels, i.e.  $S_0, S_i \sim \text{Exp}(1)$ , (6) simplifies to

$$\mathcal{L}_{I_\Phi}(\zeta) = \exp \left\{ -2\pi\lambda \int_0^\infty \frac{u}{1+|u|^\alpha/\zeta} du \right\} = e^{-\lambda C \zeta^{\frac{2}{\alpha}}} \quad (7)$$

with  $\mathcal{L}_{I_\Phi}(\zeta)$  evaluated at  $\zeta = \beta R^\alpha$  and  $C = \frac{2\pi}{\alpha} \Gamma(\frac{2}{\alpha}) \Gamma(1 - \frac{2}{\alpha})$ , with  $\Gamma(t) = \int_0^\infty x^{t-1} e^{-x} dx$  being the Gamma function. Note that  $C$  depends on the distribution of the interference power, and so for some systems, it may no longer be a function of the path loss exponent alone. For all cases considered in this paper, the integral in (6)

$$\int_{\mathbb{R}^2} 1 - E \left[ e^{-\zeta S_i |x|^{-\alpha}} \right] dx$$

where  $\zeta$  is evaluated at  $\beta R^\alpha$ , will be proportional to  $(\beta R^\alpha)^{\frac{2}{\alpha}}$ . This has the simple sphere packing interpretation that each transmission takes up an ‘‘area’’ proportional to  $(\beta^{1/\alpha} R)^2$ .

### B. The Optimal Contention Density

By now applying a small outage constraint (e.g.,  $\epsilon < .1$ ) to (5), the network just meets this constraint when

$$\mathbf{P}(SIR \geq \beta) = 1 - \epsilon = e^{-\lambda C R^2 \beta^{\frac{2}{\alpha}}} \quad (8)$$

and solving for  $\lambda$  yields the optimal contention density:

$$\lambda_\epsilon = \frac{-\ln(1 - \epsilon)}{C R^2 \beta^{\frac{2}{\alpha}}} = \frac{\epsilon}{C R^2 \beta^{\frac{2}{\alpha}}} + \Theta(\epsilon^2). \quad (9)$$

This result given in [14] and [15] can be generalized through the following Lemma.

*Lemma 1: Let the interfering transmitters form a Poisson process of intensity  $\lambda$  around a typical receiver with the outage probability being  $\mathbf{P}(SIR \leq \beta) = \mathbf{P}(\frac{\rho S_0 R^{-\alpha}}{\rho I_\Phi} \leq \beta)$  with fixed  $\rho$ ,  $\beta$ ,  $R$ , and  $\alpha$ . Suppose  $F_{S_0}^c$  takes the form*

$$F_{S_0}^c(x) = \sum_n e^{-nx} \sum_k a_{nk} x^k \quad (10)$$

for  $n, k \in \mathbb{N}$ , and suppose  $S_0$  is independent of  $I_\Phi$ , then

$$\mathbf{P}(SIR \geq \beta) = \sum_n \sum_k \left[ a_{nk} \left( -\frac{\zeta}{n} \right)^k \frac{d^k}{d\zeta^k} \mathcal{L}_{I_\Phi}(\zeta) \right]_{\zeta = n\beta R^\alpha}. \quad (11)$$

Furthermore, for a small outage constraint  $\epsilon$ , the optimal contention density is given by the first order Taylor expansion of (11) around  $\lambda \beta^{\frac{2}{\alpha}} R^2 C_\alpha = 0$ :

$$\lambda_\epsilon = \frac{K_\alpha}{C_\alpha} \frac{\epsilon}{R^2 \beta^{\frac{2}{\alpha}}}. \quad (12)$$

for

$$K_\alpha = \left[ \sum_n \sum_k a_{nk} n^{\frac{2}{\alpha} - k} \prod_{l=0}^{k-1} (l - 2/\alpha) \right]^{-1} \quad (13)$$

and  $C_\alpha (\beta R^\alpha)^{\frac{2}{\alpha}} = \int_{\mathbb{R}^2} 1 - E[e^{-\zeta S_i |x|^{-\alpha}}] dx$ .

*Proof:* The proof is presented in Appendix I. ■

This Lemma has two key contributions and several implications. The Lemma’s two contributions are (1) that it gives the exact probability of outage for any network density or target SIR (thermal noise was eliminated for convenience but could easily be reinserted) but also (2) that it gives a solution for the optimal contention density in the low outage regime. As for consequences of the Lemma, first, it reinforces the linear dependence of the optimal contention density with the outage constraint for uniformly distributed random access systems. When compared with a regular network topology,  $\epsilon$  essentially becomes a penalty factor on the area spectral efficiency achievable with random access. Second, it shows that a large class of received signal and fading distributions is amenable to a transmission capacity analysis, including a number of MIMO techniques. Third, it demonstrates that derivation of the transmission capacity consists of two components: (1) determining  $K_\alpha$  which is dependent on the received signal distribution, and (2) determining  $C_\alpha$  which is a result of the interfering signal statistics. Note that this holds in general only when the condition of independence between the received signal distribution and the interfering shot noise process is satisfied.

### III. TRANSMISSION CAPACITY IN LOS AND NLOS ENVIRONMENTS

In [14], the same Poisson network model was used but propagation was modeled with path loss only while [15] incorporated Rayleigh fading in addition to path loss. In order to characterize the effect on network capacity between these extremes, Rayleigh fading and non-fading, let the envelope of the received signal be Nakagami- $m$  distributed with integer parameter  $m$  in addition to being scaled by path loss. The Nakagami distribution includes Rayleigh as a special case ( $m = 1$ ), non-fading as a special case ( $m = \infty$ ), and provides a close parameterized fit for empirical data as well as the Ricean distribution for  $m = \frac{(K+1)^2}{(2K+1)}$  for  $K$  the Ricean factor [33]. That is, let  $S_0, S_i \sim \text{Nak}(m)$ . This allows the application of Lemma 1 as follows:

*Theorem 1: For a random access single-antenna narrow-band wireless network in Nakagami- $m$  fading for  $m \in \mathbb{N}$ , the optimal contention density with outage  $\epsilon$  is given by*

$$\lambda_\epsilon = \frac{K_{\alpha,m} \epsilon}{C_{\alpha,m} \beta^{\frac{2}{\alpha}} R^2} \quad (14)$$

where

$$K_{\alpha,m} = \left[ 1 + \sum_{k=0}^{m-2} \frac{1}{(k+1)!} \prod_{l=0}^k (l - 2/\alpha) \right]^{-1} \quad (15)$$

and

$$C_{\alpha,m} = \frac{2\pi}{\alpha} \sum_{k=0}^{m-1} \binom{m}{k} B \left( \frac{2}{\alpha} + k; m - \left( \frac{2}{\alpha} + k \right) \right). \quad (16)$$

with  $B(a, b) = \frac{\Gamma(a)\Gamma(b)}{\Gamma(a+b)}$  being the Beta function. Further, both  $K_{\alpha,m}$  and  $C_{\alpha,m}$  increase as  $\Theta(m^{\frac{2}{\alpha}})$  with

$$m^{\frac{2}{\alpha}} \leq K_{\alpha,m} \leq \Gamma(1 - 2/\alpha) m^{\frac{2}{\alpha}} \quad (17)$$

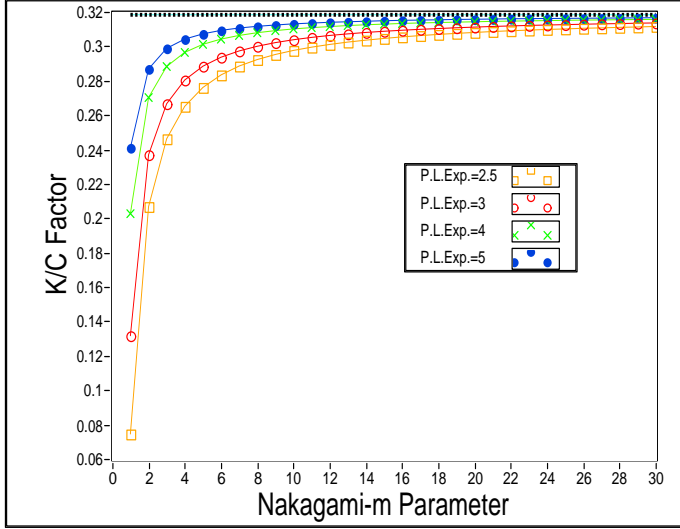


Fig. 1.  $\frac{K_{\alpha,m}}{C_{\alpha,m}} \rightarrow .318 \approx \frac{1}{\pi}$  as  $m \rightarrow \infty$  for various path loss exponents.

and

$$0 < \frac{K_{\alpha,1}}{C_{\alpha,1}} < \frac{K_{\alpha,m}}{C_{\alpha,m}} < \frac{1}{\pi} \quad (18)$$

with the upper bound approximately tight as  $m \rightarrow \infty$ .

*Proof:* The proof is presented in Appendix II. ■

It was shown in [14] that in a non-fading environment, the transmission capacity is bounded above by

$$\lambda_\epsilon \leq \frac{\epsilon}{\pi \beta^{\frac{2}{\alpha}} R^2} \quad (19)$$

and further more this upper bound is fairly tight which implies that in fact  $\lim_{m \rightarrow \infty} \frac{K_{\alpha,m}}{C_{\alpha,m}} \approx \frac{1}{\pi}$ . Fig. 1 shows the ratio  $\frac{K_{\alpha,m}}{C_{\alpha,m}}$  for various  $\alpha$  versus  $m$ . This reinforces the (rough) tightness of the upper bound in [14].

Theorem 1 bridges the gap between fading and non-fading environments and demonstrates the potentially significant gain in network capacity relative to non-fading environments. It also shows that environments with lower path loss suffer more from severe fading (when in the common practical case  $\beta > 1$ ) and improve more with a strong LOS. The distinction is particularly important for dense networks communicating with nearby neighbors which are likely to have lower path loss and a significant LOS which is in contrast to the model in [13]. The results also reveal the gains to be reaped by diversity techniques that can mitigate fading. The particular results for  $K_{\alpha,m}$  and  $C_{\alpha,m}$  will also be significant in the analysis of numerous MIMO techniques.

#### IV. SECTORIZED ANTENNAS

Now consider the same network model but with transmitters and receivers that are each equipped with  $M$  sectorized antennas. Let each antenna cover an angle of  $\frac{2\pi}{M}$  radians with an aperture gain of  $M$  for both transmitting and receiving in its sector and (potentially) with some small input/output gain outside its sector. Again let transmitters still use fixed power  $\rho$  and

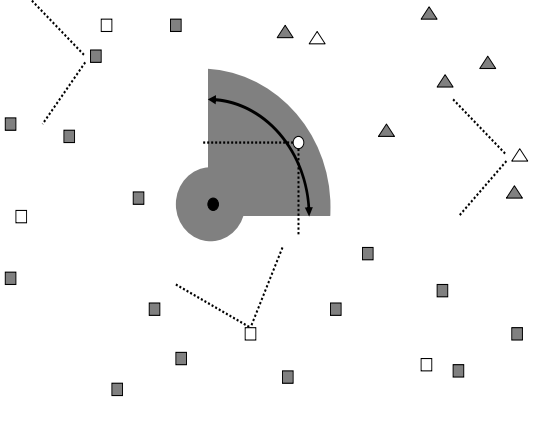


Fig. 2. Sectorized antenna model with constant sidelobe level of the receiver of interest (black dot), its intended transmitter (white dot), and the four sets of interferers:  $\Phi_1$  the interferers in the active sector transmitting toward the receiver (white triangles),  $\Phi_2$  the interferers in the active sector transmitting away from the receiver (shaded triangles),  $\Phi_3$  the interferers out of the active sector transmitting toward the receiver (white squares), and  $\Phi_4$  the interferers out of the active sector transmitting away from the receiver (shaded squares).

both the transmitter and receiver know the sector in which to communicate with their intended partner. The model can include a constant sidelobe level  $\gamma$ , where the ratio of the sidelobe level to the main lobe is  $0 \leq \gamma \leq 1$ , for out-of-sector power which is both transmitted and received by the sectorized antenna. Fig. 2 may help to visualize the model. The table conveys the power emitted by a transmitter in and out-of sector subject to constant total power  $\rho$ :

–	In sector	Out of sector	Combined
Power emitted:	$\frac{\rho}{1+\gamma(M-1)}$	$\frac{\rho\gamma(M-1)}{1+\gamma(M-1)}$	Sum: $\rho$
Sector size (rad):	$2\pi \frac{1}{M}$	$2\pi \frac{M-1}{M}$	Sum: $2\pi$
Power density:	$\frac{M/2\pi}{1+\gamma(M-1)}$	$\frac{\gamma M/2\pi}{1+\gamma(M-1)}$	Ratio: $\gamma$

Under this model, the following theorem holds:

*Theorem 2:* For a random access wireless network in which nodes have  $M$  sectorized directional antennas in Nakagami- $m$  fading with a constant (fractional) sidelobe level  $\gamma \in [0, 1]$  for out of sector power transmitted and received, the optimal contention density with outage  $\epsilon$  is given by:

$$\lambda_\epsilon = \left( \frac{M}{1 + \gamma^{\frac{2}{\alpha}} (M-1)} \right)^2 \frac{K_{\alpha,m} \epsilon}{C_{\alpha,m} \beta^{\frac{2}{\alpha}} R^2}. \quad (20)$$

where  $K_{\alpha,m}$  is given by (15) and  $C_{\alpha,m}$  by (16). Thus  $\gamma^{-\frac{4}{\alpha}}$  is an upper bound on the transmission capacity increase due to antenna sectorization.

*Proof:* We assume the fading statistics of the received signal are unchanged by the sectorized antennas, but rather are merely scaled by the emitted and received power density. That the fading statistics are unchanged is reasonable for a small to moderate number of sectors, while for very directional antennas, the scattering seen by any given sector will be reduced and no longer have the typical isotropic properties. As a result of

sectorization, four interference terms surface as follows: Let  $\Phi_1$  be the set of interferers which are in the active sector of the receiver of interest and are transmitting toward the receiver. Let  $\Phi_2$  be the set of interferers in the receiver's active sector which are not transmitting toward the receiver. Let  $\Phi_3$  be the set of interferers outside the receiver's sector which are transmitting toward the receiver. And let  $\Phi_4$  consist of those interferers transmitting away from the receiver and which are not in the receiver's sector. The independence property of the Poisson process implies these four shot noise processes are independent as well. Furthermore, the  $I_{\Phi_i}$  are each related to  $I_{\Phi}$  since they occur over disjoint subsets of the plane (i.e., a certain sector), are scaled by the combined antenna gains, and the point process of interferers is thinned according to the direction the interferers transmit. The table summarizes the interference contributions from each of these processes with  $\lambda_i$  the effective node density of the process,  $\theta_i$  the sector size over which the process occurs from the perspective of the typical receiver, and  $\psi_i$  the combined antenna gains.

–	$\lambda_i$	$\theta_i$	$\psi_i$
$I_{\Phi_1}$	$\lambda \frac{1}{M}$	$2\pi \frac{1}{M}$	$\left(\frac{M}{1+\gamma(M-1)}\right)^2$
$I_{\Phi_2}$	$\lambda \frac{M-1}{M}$	$2\pi \frac{1}{M}$	$\gamma \left(\frac{M}{1+\gamma(M-1)}\right)^2$
$I_{\Phi_3}$	$\lambda \frac{1}{M}$	$2\pi \frac{M-1}{M}$	$\gamma \left(\frac{M}{1+\gamma(M-1)}\right)^2$
$I_{\Phi_4}$	$\lambda \frac{M-1}{M}$	$2\pi \frac{M-1}{M}$	$\gamma^2 \left(\frac{M}{1+\gamma(M-1)}\right)^2$

The transforms of the shot noise processes of the  $I_{\Phi_i}$  are given by

$$\mathcal{L}_{\Phi_i}(\zeta) = \exp \left\{ -\lambda_i \theta_i \int_0^\infty 1 - E \left[ e^{-\zeta \psi_i S |x|^{-\alpha}} \right] dx \right\} \quad (21)$$

for  $\zeta = \psi_0^{-1} \beta R^\alpha$  with  $\psi_0 = \psi_1$  being the combined antenna gain between the typical receiver and its intended transmitter. Consider first the Rayleigh fading case. The outage probability at a typical receiver is given by

$$\begin{aligned} \mathbf{P}(SIR \geq \beta) &= \mathbf{P} \left( \frac{\psi_0 \rho S_0 R^{-\alpha}}{\rho \sum_{i=1}^4 I_{\Phi_i}} \geq \beta \right) \\ &= \int_0^\infty F_{S_0}^c(\psi_0^{-1} \beta R^\alpha s) f_{[I_{\Phi_1} + I_{\Phi_2} + I_{\Phi_3} + I_{\Phi_4}]}(s) \\ &= \prod_{i=1}^4 \mathcal{L}_{\Phi_i}(\zeta) |_{\zeta = \psi_0^{-1} \beta R^\alpha} \\ &= \exp \left\{ -\lambda \beta^{\frac{2}{\alpha}} R^2 C_\alpha \left( \frac{1 + \gamma^{\frac{2}{\alpha}} (M-1)}{M} \right)^2 \right\} \end{aligned} \quad (22)$$

and solving for  $\lambda$

$$\lambda_\epsilon = \left( \frac{M}{1 + \gamma^{\frac{2}{\alpha}} (M-1)} \right)^2 \frac{\epsilon}{C_\alpha \beta^{\frac{2}{\alpha}} R^2}. \quad (23)$$

Next note that  $\frac{M}{1 + \gamma^{\frac{2}{\alpha}} (M-1)} \leq \frac{1}{\gamma^{\frac{2}{\alpha}}}$  and as  $M$  becomes large, we have the limit

$$\lim_{M \rightarrow \infty} \left( \frac{M}{1 + \gamma^{\frac{2}{\alpha}} (M-1)} \right)^2 = \frac{1}{\gamma^{\frac{4}{\alpha}}}. \quad (24)$$

This results in an upper bound of  $\gamma^{-\frac{4}{\alpha}}$  on the improvement (over (14)) in optimal contention density from sectorized antennas.

If signals are Nakagami- $m$  distributed instead, since the desired and interfering signals are independent,  $C_\alpha$  can be replaced by  $C_{\alpha,m}$  and according to the transform analysis in Appendices I and II,  $K_{\alpha,m}$  appears in the numerator of (23). ■

These results firstly indicate that directional antennas increase transmission capacity by nearly a factor of  $M^2$  for low sidelobe levels. This indicates that MIMO techniques that avoid or reduce interference in an ad hoc network are highly beneficial at the physical layer. In addition there are advantages at higher network layers such as increased ability to learn the topology of the network, perform directional routing, etc; see [34] and [35] and references therein for more details. This section has characterized the potential increase in area spectral efficiency due to antenna sectorization which by itself provides greater potential and flexibility for routing and network management, but the full relationship between directional antennas and these higher layer functions is still an area of ongoing research.

However, this analysis also indicates that if for practical reasons, sidelobe levels cannot be reduced, then the sidelobes limit the potential gains even for very directional antennas. This model also suffers from very idealistic assumptions about the real propagation environment, especially since dense multipath can result in signal angle of arrival being quite different from the geographic angle to the transmitter. As pointed out in [34], real antenna patterns are far from “pie slices” and in multipath environments, static antennas are much less robust to fluctuating channels.

## V. TRANSMISSION CAPACITY OF EIGEN-BEAMFORMING NETWORKS

Dynamic beamforming is one of the most prominent multiple antenna techniques, having been employed for decades in electromagnetic detection and imaging applications. The complexity is manageable and it can be performed on any number of antennas in any configuration ([36], ch. 6). However, to be explicit since “beamforming” has become quite an overloaded term, this section uses the term to mean the following: At the receiver it refers to a coherent linear combination of the antenna outputs, while at the transmitter it refers to sending linearly weighted versions of the same signal on each antenna. Thus, unlike the previous section, no attention is paid to the specific physical pattern of energy propagation. In each case for this analysis, the weights are determined by the dominant singular vectors or eigenvectors (hence, “eigen-beamforming”) of the channel. Throughout this section it is assumed that both the transmitter and receiver have perfect channel knowledge of their own channel, but not of interfering channels. Hence, signaling strategies will maximize SNR over a specific channel but not necessarily SINR, though the analysis of the resulting interference-limited systems will ultimately ignore background thermal noise. We focus first on the vector (SIMO or MISO) channel for which eigen-beamforming is equivalent to maximal ratio transmission or combining. We then consider the general matrix (MIMO) channel for which a single datastream is sent over the dominant eigenmode.

### A. $1 \times M$ and $M \times 1$ Eigen-Beamforming

Consider first a wireless system in which all transmitters transmit with power  $\rho$  using only one antenna and receivers beamform on  $M$  antennas by coherently combining the received signals. Again, this is beamforming along the dominant (and only) eigenmode of the  $1 \times M$  channel. As shown in [26], this is equivalent to an  $M \times 1$  vector channel for which maximal ratio transmission is performed at the transmitter and one receive antenna is used. The channel model for the desired signal in a Rayleigh fading environment is a vector of i.i.d. unit variance, complex Gaussian entries scaled by the power law path loss function:  $\mathbf{h}_0|R|^{-\alpha}$  for the  $k$ th entry of  $\mathbf{h}_0$  independently  $[\mathbf{h}_0]_k \sim \mathcal{CN}(0, 1)$ , and similarly the channel between a receiver and the  $i$ th interferer is  $\mathbf{h}_i|X_i|^{-\alpha}$  with  $[\mathbf{h}_i]_k \sim \mathcal{CN}(0, 1)$ . Under this model, the following theorem holds. As in Sec. III, the theorem will be given in two parts: the first is an expression for the exact optimal contention density for small outage constraints and the second is a set of bounds that help interpret the exact results.

*Theorem 3: For a random access wireless network in which nodes transmit on a single antenna and perform maximal ratio combining with  $M$  antennas; or equivalently perform maximal ratio transmission with  $M$  antennas and receive on a single antenna; the optimal contention density under Rayleigh fading with outage constraint  $\epsilon$  is given by:*

$$\lambda_\epsilon = \frac{K_{\alpha, M} \epsilon}{C_\alpha \beta^{\frac{2}{\alpha}} R^2} \quad (25)$$

where  $K_{\alpha, M}$  is given by (15) and  $C_\alpha = C_{\alpha, 1}$  in (16). Further,  $\lambda_\epsilon$  is  $\Theta(M^{\frac{2}{\alpha}})$  and bounded by:

$$\frac{M^{\frac{2}{\alpha}} \epsilon}{C_\alpha \beta^{\frac{2}{\alpha}} R^2} \leq \lambda_\epsilon \leq \frac{\Gamma(1 - \frac{2}{\alpha}) M^{\frac{2}{\alpha}} \epsilon}{C_\alpha \beta^{\frac{2}{\alpha}} R^2}. \quad (26)$$

*Proof:* To characterize the interference seen by an  $M$ -antenna receiver that ignores interfering signals, beamforming simply to maximize its own received signal power (again thermal noise is assumed negligible), the SIR expression is given by:

$$\begin{aligned} SIR &= \frac{\frac{\rho}{M} |\mathbf{h}_0^H \mathbf{h}_0|^2 R^{-\alpha}}{\frac{\rho}{M} \sum_{X_i \in \Phi} |\mathbf{h}_0^H \mathbf{h}_i|^2 |X_i|^{-\alpha}} \\ &= \frac{\|\mathbf{h}_0\|^2 R^{-\alpha}}{\sum_{X_i \in \Phi} \left| \frac{\mathbf{h}_0^H \mathbf{h}_i}{\|\mathbf{h}_0\|} \right|^2 |X_i|^{-\alpha}}. \end{aligned} \quad (27)$$

As shown in [25], since a linear combination of Gaussian variables is again Gaussian, the product  $\frac{\mathbf{h}_0^H \mathbf{h}_i}{\|\mathbf{h}_0\|}$  is distributed as a single complex Gaussian random variable with zero mean and unit variance. Letting  $S_i = \left| \frac{\mathbf{h}_0^H \mathbf{h}_i}{\|\mathbf{h}_0\|} \right|^2$ , which is exponentially distributed, the SIR expression is

$$SIR = \frac{\|\mathbf{h}_0\|^2 R^{-\alpha}}{\sum_{X_i \in \Phi} S_i |X_i|^{-\alpha}} = \frac{\|\mathbf{h}_0\|^2 R^{-\alpha}}{I_\Phi}. \quad (28)$$

Setting  $S_0 = \|\mathbf{h}_0\|^2$  and considering the network model in Sec. II but with beamforming receivers with  $M$  antennas, the

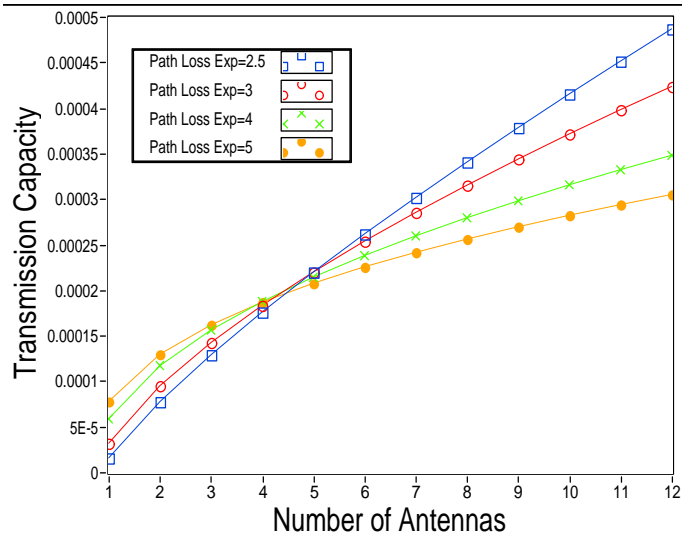


Fig. 3. Transmission capacity versus  $M$  for four path loss exponents for  $1 \times M$  MRC. Higher path loss separates transmissions spatially and is the dominant effect for smaller numbers of antennas. But with a larger number of antennas, ultimately network performance is improved more through interference robustness than spatial separation.

distribution of the received signal is now  $\chi^2$  with  $2M$  degrees of freedom. The CCDF of  $S_0$  is:

$$F_{S_0}^c(x) = e^{-x} \sum_{k=0}^{M-1} \frac{x^k}{k!}. \quad (29)$$

However, the interference has the same form as the shot noise process for the single-antenna case. If we now apply a small outage constraint and Lemma 1, we can state very simply that  $K_{\alpha, M}$  is given by (15) and  $C_\alpha = C_{\alpha, 1}$  in (16) which gives the result. As shown in (17),

$$1 \leq \frac{K_{\alpha, M}}{M^{\frac{2}{\alpha}}} \leq \Gamma(1 - 2/\alpha)$$

which indicates that

$$\begin{aligned} \frac{M^{\frac{2}{\alpha}} \epsilon}{C_\alpha \beta^{\frac{2}{\alpha}} R^2} &\leq \frac{K_{\alpha, M} \epsilon}{C_\alpha \beta^{\frac{2}{\alpha}} R^2} \leq \frac{\Gamma(1 - \frac{2}{\alpha}) M^{\frac{2}{\alpha}} \epsilon}{C_\alpha \beta^{\frac{2}{\alpha}} R^2} \\ \frac{M^{\frac{2}{\alpha}} \epsilon}{C_\alpha \beta^{\frac{2}{\alpha}} R^2} &\leq \lambda_\epsilon \leq \frac{\Gamma(1 - \frac{2}{\alpha}) M^{\frac{2}{\alpha}} \epsilon}{C_\alpha \beta^{\frac{2}{\alpha}} R^2} \end{aligned}$$

with equality to the lower bound at  $M = 1$  and approaching the upper bound with increasing  $M$ . This is due to the fact that  $C_\alpha$  is constant for all  $M$  and is bounded but monotonically increasing. ■

Theorem 3 gives a general scaling of the optimal contention density with the number of antennas, target SIR, path loss, the transmitter-receiver separation, and the outage constraint. Fig. 3 gives the transmission capacity versus  $M$  for four different path loss exponents. Fig. 4 gives the  $K_{\alpha, M}$  factor versus  $M$  for the same path loss exponents. As evident from the figures, as path loss reduces and interference becomes less attenuated by distance, the gain of the MIMO technique over the SISO case increases. However, higher path loss results in higher transmission capacity for smaller numbers of antennas since path loss helps to spatially

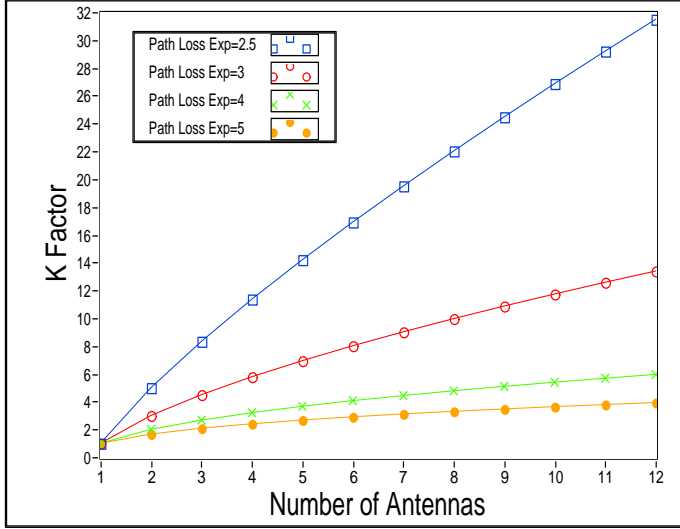


Fig. 4. The  $K_{\alpha, M}$  factor versus  $M$  for four path loss exponents for  $1 \times M$  MRC. Lower path loss results in much greater gains over the SISO case ( $M = 1$ ).

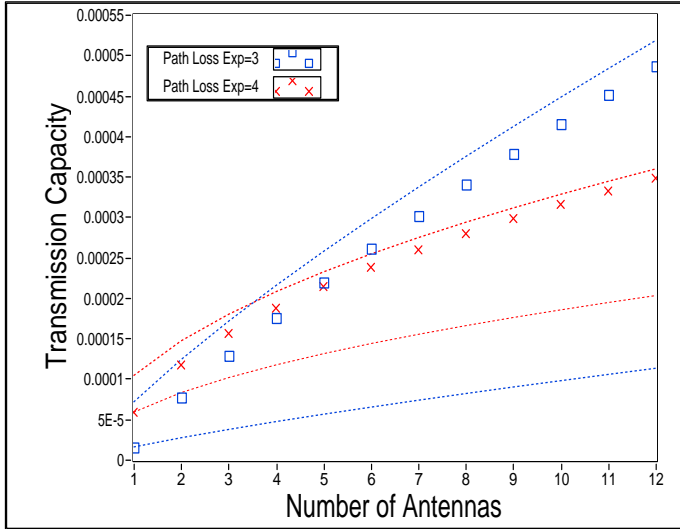


Fig. 5. Demonstration of the bounds on transmission capacity for  $1 \times M$  or equivalently  $M \times 1$  MRC. The upper bound is asymptotically tight and a good approximation for higher path loss.

separate transmissions. Fig. 5 demonstrates the relationship of the exact  $K_{\alpha, M}$  factor to the upper and lower bounds. The upper bound is both asymptotically tight and a good approximation for higher path loss.

### B. $M_t \times M_r$ MIMO Eigen-Beamforming

Now consider the same network but with nodes each equipped with  $M_t$  transmit and  $M_r$  receive antennas to perform dynamic eigen-beamforming at both transmitter and receiver ends. This extension of MRC has significant advantages even over  $1 \times M$  MRC since the diversity order increases as  $M_t M_r$  [37]. The Rayleigh fading MIMO channel is modeled as a matrix of i.i.d. zero-mean, unit-variance complex Gaussian entries scaled by path loss. The channel of the desired signal for the transmitter-receiver

pair of interest is denoted  $\mathbf{H}_{00}$ . The transmitter and receiver beamform using the input and output singular vectors  $\mathbf{v}_0$  and  $\mathbf{u}_0$ , respectively, corresponding to the maximum singular value of  $\mathbf{H}_{00}$ . This results in the received power being equal to the square of the maximum singular value  $\phi_{\max}^2$  scaled by path loss and the transmit power. Each interfering transmitter, on the other hand, beamforms to maximize received power across some other Rayleigh channel  $\mathbf{H}_{ii}$  using beamforming vector  $\mathbf{v}_i$ , and interferes at the receiver of interest through channel  $\mathbf{H}_{0i}$ . For such a network, the following bounds hold:

*Theorem 4:* For a random access wireless network in which nodes perform maximal ratio transmission and combining on  $M_t$  and  $M_r$  antennas respectively, for small outages the optimal contention density is bounded by:

$$\frac{\max\{M_t, M_r\}^{\frac{2}{\alpha}} \epsilon}{C_\alpha R^2 \beta^{\frac{2}{\alpha}}} \leq \lambda_\epsilon \leq \frac{\Gamma(1 - \frac{2}{\alpha})(M_t M_r)^{\frac{2}{\alpha}} \epsilon}{C_\alpha R^2 \beta^{\frac{2}{\alpha}}} \quad (30)$$

for  $C_\alpha = C_{\alpha, 1}$  given in (16).

*Proof:* To begin, the SIR expression for this model is

$$SIR = \frac{\rho \phi_{\max}^2 R^{-\alpha}}{\rho \sum_{X_i \in \Phi} |X_i|^{-\alpha} |\mathbf{u}_0^H \mathbf{H}_{0i} \mathbf{v}_i|^2}. \quad (31)$$

Note that  $\mathbf{u}_0$ ,  $\mathbf{H}_{0i}$ , and  $\mathbf{v}_i$  are all independent. As discussed in [27], the full product  $\mathbf{u}_0^H \mathbf{H}_{0i} \mathbf{v}_i$  is distributed as a single zero-mean, unit-variance, complex Gaussian variable since the inner product of a vector i.i.d. complex Gaussian variables with an arbitrary unit vector is a single complex Gaussian variable. This simplifies the SIR expression to

$$SIR = \frac{\phi_{\max}^2 R^{-\alpha}}{I_\Phi}. \quad (32)$$

with the distribution of the interference unchanged from the single antenna Rayleigh fading case. Again neglecting thermal noise, the received and interfering signals are independent and  $C_\alpha = C_{\alpha, 1}$  in (16) by equivalence of the shot noise processes.

As for the received signal, note that the CCDF of the square of the maximum singular value of the desired channel (or equivalently the largest eigenvalue of a complex Wishart matrix), has been reported by Kang and Alouini [26] (originally given by Khatri [38]):

$$F_{\phi_{\max}^2}^c(x) = 1 - \frac{|\Psi(x)|}{\prod_{k=1}^q \Gamma(q - k + 1) \Gamma(s - k + 1)}$$

where  $|\cdot|$  denotes a determinant,  $q = \min\{M_t, M_r\}$ ,  $s = \max\{M_t, M_r\}$ , and the entries of the  $q \times q$  matrix  $\Psi(x)$  are given by

$$\{\Psi(x)\}_{i,j} = \gamma(s - q + i + j - 1, x), \quad i, j = 1, \dots, q$$

where  $\gamma(\cdot, \cdot)$  is the lower incomplete gamma function. Recall

$$\gamma(n, x) = (n-1)! \left( 1 - e^{-x} \sum_{k=0}^{n-1} \frac{x^k}{k!} \right), \quad n \in \mathbb{N}.$$

This now facilitates the application of Lemma 1 yielding the outage probability and the optimal contention density, which will again have the form:

$$\lambda_\epsilon = \frac{K_{\alpha, M_t, M_r}^{mrt} \epsilon}{C_\alpha R^2 \beta^{\frac{2}{\alpha}}}.$$

We are unable to give a general expression for  $K_{\alpha, M_t, M_r}^{mrt}$  since the explicit sum-of-exponentials-and-polynomials form for  $F_{\phi_{\max}^2}^c$  is not known. However, it is known that the largest squared singular value is bounded by [39]:

$$\|\mathbf{H}_{00}\|_F^2 \geq \phi_{\max}^2 \geq \frac{\|\mathbf{H}_{00}\|_F^2}{\min\{M_t, M_r\}}.$$

Since  $\|\mathbf{H}_{00}\|_F^2$  is  $\chi^2$  with  $2M_t M_r$  degrees of freedom this is equivalent to a particular MRC case in (25) and (26) indicating that

$$K_{\alpha, M_t, M_r}^{mrt} \leq K_{\alpha, (M_t M_r)} \leq \Gamma(1 - 2/\alpha)(M_t M_r)^{\frac{2}{\alpha}} \quad (33)$$

so that

$$\lambda_\epsilon \leq \frac{\Gamma(1 - \frac{2}{\alpha})(M_t M_r)^{\frac{2}{\alpha}} \epsilon}{C_\alpha R^2 \beta^{\frac{2}{\alpha}}}. \quad (34)$$

Furthermore, a lower bound can be obtained from (26) as

$$\begin{aligned} K_{\alpha, M_t, M_r}^{mrt} &\geq \frac{K_{\alpha, (M_t M_r)}}{\min\{M_t, M_r\}^{\frac{2}{\alpha}}} \\ &\geq \frac{(M_t M_r)^{\frac{2}{\alpha}}}{\min\{M_t, M_r\}^{\frac{2}{\alpha}}} \\ &= \max\{M_t, M_r\}^{\frac{2}{\alpha}} \end{aligned} \quad (35)$$

so that

$$\lambda_\epsilon \geq \frac{\max\{M_t, M_r\}^{\frac{2}{\alpha}} \epsilon}{C_\alpha R^2 \beta^{\frac{2}{\alpha}}}. \quad (36)$$

Since  $K_{\alpha, M_t, M_r}^{mrt}$  cannot be given explicitly for arbitrary  $M_t$  and  $M_r$  at present, consider as an example the case  $M_t = M_r = 2$  for which

$$\begin{aligned} F_{\phi_{\max}^2}^c(x) &= 1 - (\gamma(3; x)\gamma(1; x) - \gamma^2(2; x)) \\ &= 2e^{-x} - e^{-2x} + x^2 e^{-x}. \end{aligned}$$

Applying Lemma 1 for small outages:

$$\mathbf{P}(SIR < \beta) \approx \lambda C_\alpha R^2 \beta^{\frac{2}{\alpha}} \left( 2 - 2^{\frac{2}{\alpha}} - \frac{2}{\alpha} \left( 1 - \frac{2}{\alpha} \right) \right) \quad (37)$$

with the optimal contention density being:

$$\lambda_\epsilon = \frac{\epsilon}{C_\alpha R^2 \beta^{\frac{2}{\alpha}}} \cdot \frac{1}{2 - 2^{\frac{2}{\alpha}} - \frac{2}{\alpha} \left( 1 - \frac{2}{\alpha} \right)}. \quad (38)$$

Through Monte Carlo simulation we find the mean of  $\phi_{\max}^2$  of an  $M_t \times M_r$  channel matrix to be  $\approx 2$ -3 times  $\max\{M_t, M_r\}$ . This leads to the conjecture that for moderately large numbers of antennas (e.g.,  $M_t, M_r > 3$ ), neither the upper nor lower bounds given here are particularly tight. But it does imply that the larger number of antennas at *either* transmitter or receiver yields the dominant increase in transmission capacity when beamforming along the dominant spatial mode.

Fig. 6 depicts both  $K_{\alpha, M}$  and for the square channel case  $M = M_t = M_r$ ,  $K_{\alpha, M}^{mrt}$  for various  $M$ ,  $\alpha$ . Again  $K_{\alpha, M}^{mrt} \rightarrow 1$  with increasing  $\alpha$ . This implies that as  $\alpha$  becomes large, nodes are already spatially separated through path loss, and spatial diversity yields less improvement over the single antenna case. Conversely, when interference is higher, spatial diversity techniques yield greater gains over single-antenna systems.

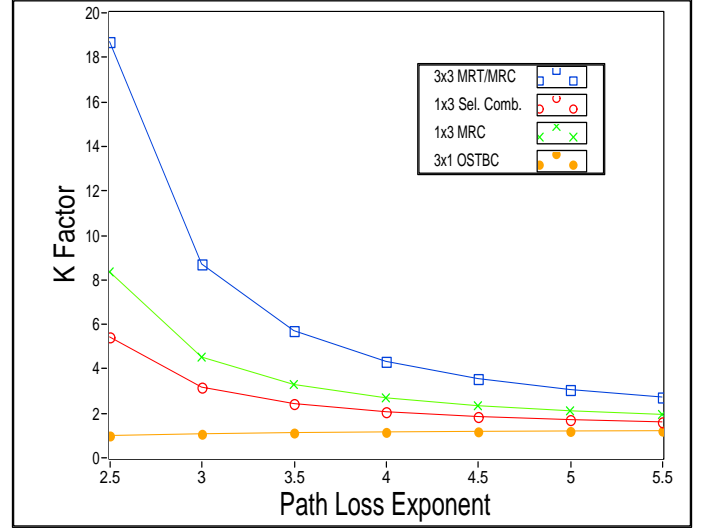


Fig. 6.  $K_{\alpha, 3}^{mrt}$  ( $3 \times 3$  MRT/MRC),  $K_{\alpha, 3}$  ( $1 \times 3$  MRC),  $K_{\alpha, M}^{sc}$  ( $1 \times 3$  selection combining), and  $\frac{K_{\alpha, M_t}}{C_{\alpha, M_t}} C_{\alpha, 1}$  ( $3 \times 1$  OSTBC) versus  $\alpha$  for various  $M$ . The factor for OSTBCs is the only which increases (slightly) with increasing path loss since interference reduces. (The factor  $C_{\alpha, 1}$  is a normalizing factor for fair comparison with other techniques and the SISO case for which  $K = 1$ .)

We also point out that the expression for  $F_{\phi_{\max}^2}^c$  in Rayleigh fading channels, repeated above from [26], is given for any number of antennas at either the transmitter or receiver. The result is always a sum of terms of the form  $x^k e^{-nx}$  so that the Laplace transform method used here may be applied for systems with any number of antennas. The expression in [26] also includes the SIMO (or MISO) case developed earlier as a special case. For larger numbers of antennas especially, there also remains the question if spatial multiplexing has a place. While this is left for future investigation, it should be noted that the form of the joint distribution of the eigenvalues of Wishart matrices given in [23] indicates that the Laplace transform method can be extended to the spatial multiplexing case. A key obstacle at present is that several key eigenvalue distributions are not known in simple sum of  $x^k e^{-nx}$  term forms.

## VI. TRANSMISSION CAPACITY OF OSTBC NETWORKS

Orthogonal space-time block coding has been one of the more quickly accepted transmit diversity techniques for several good reasons. First, OSTBCs achieve full diversity in point-to-point links without requiring channel state information at the transmitter. Second, an optimum receiver design is simply a matched filter without any need for joint decoding of multiple symbols (error correction codes notwithstanding). Furthermore, space-time coding results in far less variability in the effective channel, greatly reducing the frequency and duration of deep fades. However, there is another source of effective channel instability, particularly in decentralized networks, which is cochannel interference. In light of the results on reduced fading as well as MRT/MRC earlier in this paper, for which the latter results in much greater network improvement, it is unclear how OSTBCs compare in a decentralized, interference-limited environment and warrants further investigation.

Specific codes are characterized by the number of transmit antennas used ( $M_t$ ), the number of time slots used ( $N$ ), and the number of independent data symbols sent ( $N_s$ ) [40]. Again  $M_r$  denotes the number of receive antennas but this has no effect on the code structure. However, it will also be necessary to characterize OSTBCs by the number of time slots over which each symbol is repeated ( $N_r$ ). Two examples from [41] are given below in matrix form where each row corresponds to a transmitting antenna, and each column to a time slot:

$$\mathbf{F}_1 = \begin{bmatrix} s_1 & s_2^* \\ s_2 & -s_1^* \end{bmatrix}, \mathbf{F}_2 = \begin{bmatrix} s_1 & 0 & s_2 & -s_3 \\ 0 & s_1 & s_3^* & s_2^* \\ -s_2^* & -s_3 & s_1^* & 0 \end{bmatrix}$$

The first code above is the familiar Alamouti code (for which  $M_t = N = N_s = N_r = 2$ ) and the second is an OSTBC known for  $M_t = 3$  (with  $N = 4$ ,  $N_s = 3$ , and  $N_r = 3$ ).

*Theorem 5: For a random access wireless network in which transmitting nodes use orthogonal space-time block codes with  $M_t$  transmit antennas and code parameter  $N_r$  and receiving nodes perform maximal ratio combining with  $M_r$  antennas in Rayleigh fading, the optimal contention density under the outage constraint  $\epsilon$  is given by:*

$$\lambda_\epsilon = \frac{K_{\alpha, M_t M_r} \epsilon}{C_{\alpha, N_r} \beta^{\frac{2}{\alpha}} R^2} \quad (39)$$

where  $K_{\alpha, M_t M_r}$  is given by (15) and  $C_{\alpha, N_r}$  in (16). Further,  $\lambda_\epsilon$  is  $\Theta(M_r^\alpha)$ :

$$\frac{M_r^{\frac{2}{\alpha}} \epsilon}{C_{\alpha, 1} \beta^{\frac{2}{\alpha}} R^2} \leq \lambda_\epsilon \leq \frac{M_r^{\frac{2}{\alpha}} \epsilon}{\pi \beta^{\frac{2}{\alpha}} R^2} \quad (40)$$

*Proof:* For the received signal, since detection decouples for OSTBCs [42] over the  $N_r$  time slots as well as  $M_r$  antennas, the received amplitude is  $\|\mathbf{H}_0\|_F^2$  for each symbol [42], where  $\mathbf{H}_0$  is the  $M_r \times M_t$  complex Gaussian channel. The distribution of  $\|\mathbf{H}_0\|_F^2$  is  $\chi^2$ , just as with MRC, but with  $2M_t M_r$  degrees of freedom. So applying Lemma 1, the  $K$  factor is  $K_{\alpha, M}$  in (15) for  $M = M_t M_r$ .

The interference seen by an OSTBC processing system is more complicated, however. To determine the distribution of  $S_i$ , consider the expression for the interference term from a single interferer at the time of detection:

$$|X_i|^{-\alpha} S_i = |X_i|^{-\alpha} \sum_{k=1}^{N_r} \frac{\mathbf{h}_0^H \mathbf{h}_i^{(k)}}{\|\mathbf{h}_0\|} s_i^{(k)} = |X_i|^{-\alpha} \sum_{k=1}^{N_r} S_i^{(k)} \quad (41)$$

where  $\mathbf{h}_0 = \text{vec}(\mathbf{H}_0)$  and  $\mathbf{h}_i^{(k)}$  is a permutation of the entries in  $\text{vec}(\mathbf{H}_i)$  depending on the block coding structure. Since desired symbols are repeated  $N_r$  times, each  $S_i$  is a sum  $N_r$  terms  $S_i^{(k)}$  each of which is exponentially distributed though not independent. In a strict sense, this violates the independence of  $S_0$  and  $S_i$  required by Lemma 1. However, as in [43], we assume rough independence of received and interfering signal statistics, with the statistics of the sum of  $S_i^{(k)}$  nearly indistinguishable from a Gamma distribution independent of  $S_0$  being justified through simulation.

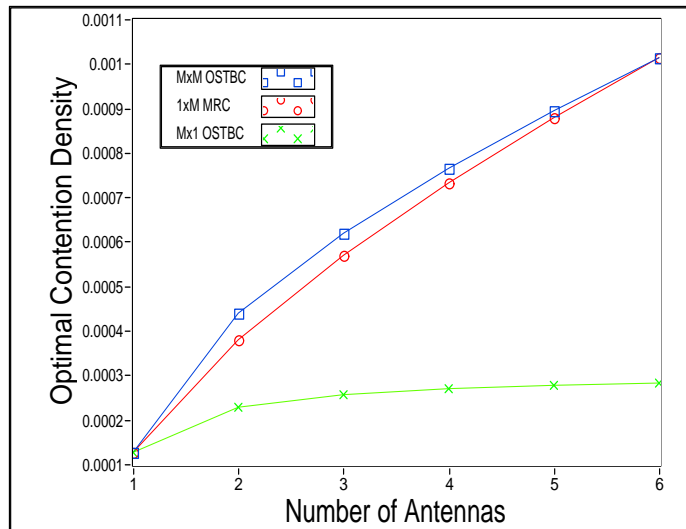


Fig. 7. Comparison of the optimal contention density for  $M \times M$  OSTBC/MRC,  $1 \times M$  MRC, and  $M \times 1$  OSTBC respectively. The optimal contention density is nearly identical to receiver MRC only and does not improve much for large numbers of transmit antennas over the single antenna case without receive beamforming.

Since the Gamma distribution is the same mark distribution encountered for Nakagami- $m$  fading interferers,  $C_{\alpha, N_r}$  is given by (16). As shown before, the factor increases with  $N_r^{\frac{2}{\alpha}}$  indicating that repeating the symbols introduces more cochannel interference. Again applying Lemma 1 for small outages

$$\lambda_\epsilon = \frac{K_{\alpha, M_t M_r} \epsilon}{C_{\alpha, N_r} R^2 \beta^{\frac{2}{\alpha}}} \quad (42)$$

where as  $M_r$  and  $M_t$  grow large,

$$\begin{aligned} \lambda_\epsilon &\leq \frac{(M_t M_r)^{\frac{2}{\alpha}} \epsilon}{\pi N_r^{\frac{2}{\alpha}} R^2 \beta^{\frac{2}{\alpha}}} \\ &= \frac{M_r^{\frac{2}{\alpha}} \epsilon}{\pi R^2 \beta^{\frac{2}{\alpha}}} \end{aligned} \quad (43)$$

for most practical block codes since  $M_t = N_r$ , which is the best case. For the lower bound, we simply ignore the change in the constant  $C_{\alpha, N_r}$  substituting  $C_{\alpha, 1}$  which is greater than  $\pi$ . (That is, let  $K_{\alpha, M}$  increase but not  $C_{\alpha, N_r}$ ). ■

The primary insight from the analysis of OSTBCs is that in an environment of significant cochannel interference, they accomplish little. As is evident from the bounds, the number of receive antennas is the primary factor in network performance. While block codes harden the channel resulting in a network performance gain equivalent to that gained from reducing fading, they also tend to amplify interference since symbols are repeated. When symbols are repeated multiple times from the same antenna, as in some orthogonal designs, this effect is worsened so that  $N_r = M_t$  is the best case. Furthermore, even though power is split between simultaneously transmitted symbols, the transmit antennas become multiple independent interference sources for other nodes in the network. Furthermore, OSTBCs take a hit in the data rate for any code beside Alamouti's. So for a larger number

of antennas, OSTBCs are typically inferior to other schemes and are likely not worth even the slight added complexity.

Fig. 7 compares the optimal contention density for  $M \times 1$  OSTBCs for which the receiver receives on only one antenna,  $M \times M$  OSTBCs for which the receiver performs MRC on  $M$  antennas in addition to the transmit block coding, as well as  $1 \times M$  MRC without block coding. The figure shows the optimal contention density for  $\alpha = 3$ , target SINR 4.77dB, and transmitter-receiver separation 10m. First, there is little gain over simply performing MRC in contention density. But what is not shown is that for the number of antennas larger than two, the transmission capacity for  $M \times M$  OSTBCs actually falls below the MRC curve since it must use a reduced rate code. If only one receive antenna is used, then for any number of transmit antennas beyond two, there is essentially no gain when code rate is taken into account. This confirms that the primary source of gain is at the receiver and that for any system beyond  $2 \times 2$ , it would be more profitable to simply select one antenna (perhaps through diversity selection) and operate in the  $1 \times M$  MRC mode.

## VII. TRANSMISSION CAPACITY OF SELECTION DIVERSITY AND COMBINING NETWORKS

A fundamental characteristic of MIMO fading channels is that due to polarization, pattern diversity, or spatial separation, one or more antenna elements may be receiving above average signal strength. Simply selecting the best often has the practical advantage over more sophisticated combining schemes of simpler implementation, or less expensive hardware. There are a variety of ways to perform antenna selection, and antenna selection can be used in conjunction with other diversity techniques. As an example let the transmitter operate one antenna and the receiver select one of  $M$  which has the best instantaneous channel with i.i.d. Rayleigh fading between all antennas. In this case,

$$F_{S_0}^c(x) = 1 - (1 - e^{-x})^M = \sum_{k=1}^M \binom{M}{k} (-1)^{k+1} e^{-kx} \quad (44)$$

and the interference fading channels  $S_i$  remain exponentially distributed. This can be extended by considering a system that selects the best pair of antennas (one transmit and one receive) from among  $M_t$  transmit and  $M_r$  receive antennas. The parameter  $M$  in (44) is simply replaced by  $M_t M_r$ . Here the full matrix channel is  $\mathbf{H}_{00}$  as in Sec. V-B from which the element with the largest magnitude is selected. Applying Lemma 1 produces the following theorem that characterizes the gain from selection diversity:

*Theorem 6: For a random access wireless network in which nodes perform selection diversity/combining by selecting the best pair among  $M_t$  transmit and  $M_r$  receive antennas in Rayleigh fading, the optimal contention density under the outage constraint  $\epsilon$  is given by:*

$$\lambda_\epsilon = \frac{K_{\alpha, M^2}^{sc}}{C_\alpha} \frac{\epsilon}{\beta_\alpha^{\frac{2}{\alpha}} R^2} \quad (45)$$

for  $M^2 = M_t M_r$  and

$$K_{\alpha, M^2}^{sc} = \left[ \sum_{k=1}^{M^2} \binom{M^2}{k} (-1)^{k+1} k^{\frac{2}{\alpha}} \right]^{-1} \quad (46)$$

and  $C_\alpha = C_{\alpha, 1}$  in (16).

*Proof:* This is given by simply substituting the coefficients in (44) into Lemma 1 and noting that the statistics of the interference are identical to the SISO case for any pair of antennas. ■

There are a number of other distributions resulting from antenna selection that can be considered. For example, in an  $M_r \times M_t$  system performing MRC at the receiver, one transmit antenna may be selected which has the largest magnitude vector channel to the intended receiver. The distribution of the interference after MRC processing will remain the same but  $S_0$  will have

$$\begin{aligned} F_{S_0}^c(x) &= 1 - \left( 1 - e^{-x} \sum_{k=0}^{M_r-1} \frac{x^k}{k!} \right)^{M_t} \\ &= \sum_{m=1}^{M_t} e^{-mx} \sum_{k=0}^{M_t(M_r-1)} a_{mk} x^k \end{aligned} \quad (47)$$

for

$$a_{mk} = (-1)^{M_t+m} \binom{M_t}{m} \sum_{i=0}^k \prod_{j=0}^i \frac{1}{j!}. \quad (48)$$

From Lemma 1 we have

$$K_{\alpha, M_t, M_r} = \left[ \sum_{m=1}^{M_t} \sum_{k=0}^{M_t(M_r-1)} m^{\frac{2}{\alpha}-k} a_{mk} \prod_{l=0}^k (l - 2/\alpha) \right]^{-1} \quad (49)$$

which specifies the optimal contention density as well. Fig. 8 compares the gain in transmission capacity for a number of systems versus the number of antennas, including MRT/MRC, OSTBCs, as well as two kinds of selection diversity/combining: one in which the transmitter transmits on one antenna and the receiver selects the best of its own antennas, and the second in which the receiver and transmitter jointly select the best pair of single antennas. Clearly antenna selection can significantly enhance network performance since it improves the typical channel without amplifying interference. Interestingly, for a  $2 \times 2$  system, selecting the best of four  $1 \times 1$  configurations is superior to  $1 \times 2$  MRC without any selection. Of course, as the number of antennas becomes large, obtaining  $M^2$  statistically independent pairs is difficult, and array gain quickly becomes superior in terms of network performance. Still, Theorem 6 implies that antenna selection may be a desirable tradeoff in terms of performance and complexity.

## VIII. SIMULATION RESULTS AND DISCUSSION

### A. Numerical Simulation

A Monte Carlo simulation of 2 million network realizations was performed in LabVIEW to verify the theoretical predictions for the optimal contention density. In Figs. 9 and 10, the optimal contention density is plotted versus outage probability for small outages, which is generally the region of interest for practical systems. In particular, they confirm the linear relationship between outage probability and optimal contention density in the low outage regime. For larger outage probabilities, the higher order polynomial factor will result in a more dramatic gain over single-antenna systems, though in a region of arguably less practical significance. A target SIR of 3 (4.77 dB) was used with a path

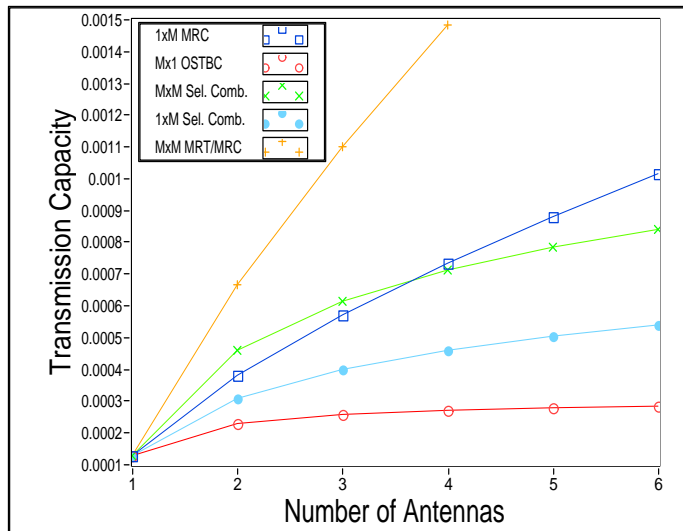


Fig. 8. Comparison of the transmission capacity for MRT, MRC, OSTBC, and selection combining. Note that  $M \times M$  OSTBC/MRC is nearly identical to the  $1 \times M$  MRC case. Also note that  $M \times M$  selection combining means selecting the best pair of transmitting and receiving antennas (one of each).

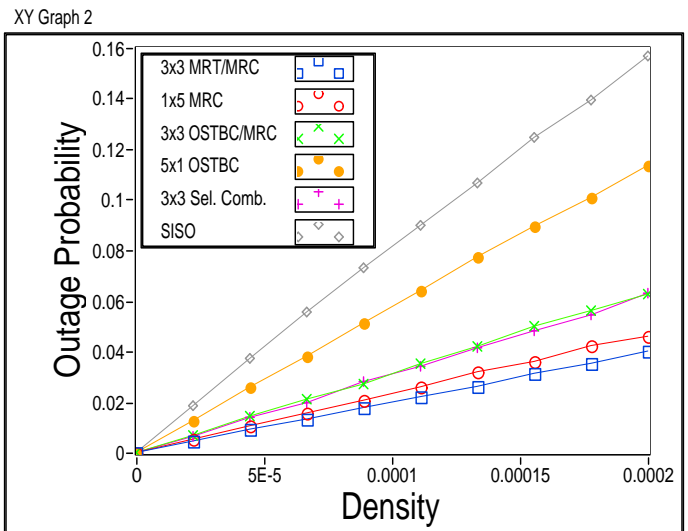


Fig. 10. Demonstration of the gains of several MIMO systems with 6 total antennas. Note that lower curves indicate better performance since the curves are versus outage probability.

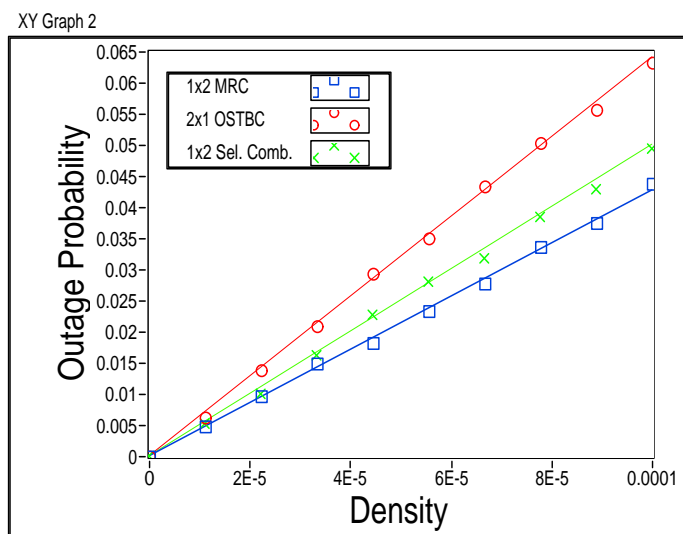


Fig. 9. Demonstration of the gains of several MIMO systems with 3 total antennas with a comparison of simulated (marked points) and theoretical performance (solid lines). Note that lower curves indicate better performance since the curves are versus outage probability.

loss exponent of 3, a transmitter-receiver separation of 10m, and no background noise power. The  $1 \times 2$  and  $1 \times 3$  curves are equivalent for transmit only or receive only beamforming systems. The curves for 6 total antennas also confirm the findings of [26] that splitting the antennas evenly between transmitter and receiver results in the best performance in the presence of cochannel interference. Note that  $5 \times 1$  OSTBCs perform worst and that  $3 \times 3$  selection combining means selecting the best pair of antennas (one transmit and one receive).

## B. Discussion

We now take a moment to discuss the physical significance of the results obtained. We first note that for a network with nodes beamforming in the SIMO or MISO case, we see the transmission capacity scales with  $M^{\frac{2}{\alpha}}$  which is the same scaling seen by DS-CDMA networks if  $M$  is the spreading factor instead of the number of antennas. In [14], this scaling was derived from the fact that the spreading factor reduced the required SIR by a factor  $M$ :

$$\begin{aligned} \lambda &\propto \frac{\epsilon}{(\beta/M)^{\frac{2}{\alpha}} R^2} \\ &= M^{\frac{2}{\alpha}} \frac{\epsilon}{\beta^{\frac{2}{\alpha}} R^2}. \end{aligned}$$

Since an array of  $M$  antennas amplifies the received signal by  $M$  on average, the scaling of SIMO or MISO beamforming systems follows the same interpretation as the DS-CDMA result, though without the loss in data rate incurred by spreading. However, as in the case of OSTBCs, there is also a small gain attributable to channel hardening.

This interpretation carries over to the general MIMO beamforming case in which we conjecture that the optimal contention density increased at least (but roughly) with  $\max\{M_t, M_r\}^{\frac{2}{\alpha}}$  since increasing  $\min\{M_t, M_r\}$  statistically increases the total energy in the MIMO channel but not much in the maximum mode. Further this implies the practical advantage of using more antennas at the receiver to achieve most of the network performance gains of beamforming while reducing channel feedback, channel sounding overhead, and transmitter hardware.

While the gain in the dynamic beamforming case is substantial, it appears to be significantly less than that obtained in the ideal sectorized antenna model. This highlights the great difference between modeling perfect orthogonality between signal and interference, versus a slight leakage. With even a slight leakage, the behavior of the system changes significantly.

## IX. CONCLUSION

In this paper, the performance of random access ad hoc networks employing a number of spatial diversity techniques was determined. Exact outage probabilities were derived for random wireless networks as well as optimal contention densities for small outage constraints for a large class of received signal distributions. These distributions include those applicable for nodes employing maximal ratio transmission/combining, orthogonal space-time block coding, selection diversity/combining, and static beamforming with sectorized antennas. The improvement in transmission capacity for Nakagami- $m$  fading channels in which fading is reduced were also given and shown to be equivalent to the small gains due to space-time codes. The results show a significant improvement in transmission capacity for sectorized antennas and beamforming systems, a lesser but still appreciable gain for selection combining systems, and marginal gains at best for space-time block coded systems. Gains are higher for beamforming and selection combining systems when interference is more severe both when node density increases and under lower path loss, while the opposite is true for space-time block coded systems. In general it was found that diversity techniques employed at the receiver offer the most practical benefits. Left as future research are the enhancements achievable from spatial multiplexing, multiuser MIMO techniques, and the combined effect of MIMO at the physical layer for scheduling, routing, and network management applied to ad hoc networks.

### APPENDIX I PROOF OF LEMMA 1

Define the PDF of  $I_\Phi$

$$f_{I_\Phi}(t) = d\mathbf{P}(I_\Phi \leq t).$$

Define a transform of  $f_{I_\Phi}(t)$  using CCDF  $F_S^c(t)$  as

$$\mathcal{G}_{I,S}(s) = \int_0^\infty F_S^c(st) f_{I_\Phi}(t) dt.$$

The probability of successful transmission can be expressed as

$$\begin{aligned} \mathbf{P}(SIR \geq \beta) &= \mathbf{P}\left(\frac{\rho SR^{-\alpha}}{\rho I_\Phi} \geq \beta\right) = \mathbf{P}(S \geq \beta R^\alpha I_\Phi) \\ &= \int_0^\infty F_S^c(st) f_{I_\Phi}(t) dt = \mathcal{G}_{I,S}(s) \Big|_{s=\beta R^\alpha} \end{aligned} \quad (50)$$

When  $S \sim \text{Exp}(1)$ ,  $F_S^c(t) = e^{-t}$  so that the Laplace transform of  $f_{I_\Phi}(t)$  is

$$\begin{aligned} \mathcal{G}_{I,S}(s) &= \int_0^\infty F_S^c(st) f_{I_\Phi}(t) dt \\ &= \mathcal{L}\{f_{I_\Phi}(t)\}(s) = \mathcal{L}_{I_\Phi}(s), \end{aligned} \quad (51)$$

and the transmission success probability is expressible in terms of the Laplace transform with argument  $s = \beta R^\alpha$ . Next suppose

$$F_S^c(t) = \sum_n e^{-nt} \sum_k a_{nk} t^k,$$

then the transform of  $f_{I_\Phi}(t)$  using CCDF  $F_S^c(t)$  is

$$\begin{aligned} \mathcal{G}_{I,S}(s) &= \int_0^\infty F_S^c(st) f_{I_\Phi}(t) dt \\ &= \int_0^\infty \left( \sum_n e^{-nst} \sum_k a_{nk} (st)^k \right) f_{I_\Phi}(t) dt \end{aligned} \quad (52)$$

$$= \sum_n \sum_k a_{nk} s^k \left( \int_0^\infty e^{-nt} t^k f_{I_\Phi}(t) dt \right) \quad (53)$$

$$= \sum_n \sum_k a_{nk} s^k \mathcal{L}\{t^k f_{I_\Phi}(t)\}(ns) \quad (54)$$

$$= \sum_n \sum_k a_{nk} (-s)^k \frac{d^k}{d(ns)^k} \mathcal{L}_{I_\Phi}(ns) \quad (55)$$

$$= \sum_n \sum_k \left[ a_{nk} \left( -\frac{\zeta}{n} \right)^k \frac{d^k}{d\zeta^k} \mathcal{L}_{I_\Phi}(\zeta) \right]_{\zeta=n\beta R^\alpha} \quad (56)$$

where the Laplace transform property

$$t^n f(t) \longleftrightarrow (-1)^n \frac{d^n}{ds^n} \mathcal{L}\{f(t)\}(s)$$

was used in (54).

To derive (13), the derivatives of  $\mathcal{L}_{I_\Phi}$  are needed and they are given by

$$\frac{d^p}{d\zeta^p} \mathcal{L}_{I_\Phi}(\zeta) = \frac{e^{-\lambda \zeta^{\frac{2}{\alpha}} C_\alpha}}{(-\zeta)^p} \sum_{k=1}^p \left( \lambda \zeta^{\frac{2}{\alpha}} C_\alpha \frac{2}{\alpha} \right)^k (-1)^k \Upsilon_{p,k} \quad (57)$$

where

$$\begin{aligned} \Upsilon_{p,k} &= \sum_{\delta_j \in \text{comb}\left(\binom{p-1}{p-k}\right)} \prod_{l_{ij} \in \delta_j} \left( \frac{2}{\alpha} (l_{ij} - i + 1) - l_{ij} \right) \\ & \quad i = 1, 2, \dots, |\delta_j|, j = 1, 2, \dots, \binom{p-1}{p-k} \end{aligned}$$

Here we define  $\text{comb}\left(\binom{a}{b}\right)$  as the set of all subsets of the natural numbers  $\{1, 2, \dots, a\}$  of cardinality  $b$  with distinct elements, i.e.,  $\text{comb}\left(\binom{a}{b}\right)$  is the set of combinations of  $\{1, 2, \dots, a\}$  taken  $b$  at a time. Thus there are  $\binom{a}{b}$  subsets in  $\text{comb}\left(\binom{a}{b}\right)$  each with  $b$  elements and the  $\delta_j$  each constitute one such subset. By convention  $\binom{a}{0} = 1$  and the zeroth derivative of a function is the function itself.

Forming the first order Taylor expansion for the  $p$ th derivative around the argument  $\kappa = \lambda \beta^{\frac{2}{\alpha}} R^2 C_\alpha = 0$ , first note that any term with  $\kappa^k$  for  $k > 1$  can be discarded so that  $\frac{d^p}{d\zeta^p} \mathcal{L}_{I_\Phi}(\zeta) \Big|_{\zeta=\beta R^\alpha}$  reduces to

$$\begin{aligned} \frac{d^p}{d\zeta^p} \mathcal{L}_{I_\Phi}(\zeta) &= (-1)^{p+1} \frac{e^{-\lambda \zeta^{\frac{2}{\alpha}} C_\alpha}}{\zeta^p} \lambda \zeta^{\frac{2}{\alpha}} C_\alpha (2/\alpha) \Upsilon_{p,1} + \Theta(\kappa^2) \\ &= (-1)^p e^{-\lambda \zeta^{\frac{2}{\alpha}} C_\alpha} \lambda \zeta^{\frac{2}{\alpha}-p} C_\alpha \prod_{l=0}^{p-1} (l - 2/\alpha) \\ & \quad + \Theta(\kappa^2) \\ &= (-1)^p \lambda \zeta^{\frac{2}{\alpha}-p} C_\alpha \prod_{l=0}^{p-1} (l - 2/\alpha) + \Theta(\kappa^2) \end{aligned} \quad (58)$$

where the small error terms are the result of the Taylor expansion. Thus a term from (11) becomes:

$$a_{nk} \left( -\frac{\zeta}{n} \right)^k \frac{d^k}{d\zeta^k} \mathcal{L}_{I_\Phi}(\zeta) = a_{nk} n^{\frac{2}{\alpha}-k} \lambda \zeta^{\frac{2}{\alpha}} C_\alpha \prod_{l=0}^{k-1} (l - 2/\alpha) + \Theta(\kappa^2)$$

so that the outage probability is given by

$$\begin{aligned} \mathbf{P}(SIR \leq \beta) &= \lambda \zeta^{\frac{2}{\alpha}} C_\alpha \sum_n \sum_k a_{nk} n^{\frac{2}{\alpha}-k} \prod_{l=0}^{k-1} (l - 2/\alpha) \\ &\quad + \Theta(\kappa^2) \\ &= \lambda \zeta^{\frac{2}{\alpha}} \frac{C_\alpha}{K_\alpha} + \Theta(\kappa^2) = \epsilon \end{aligned}$$

and with  $\zeta = \beta R^\alpha$  and  $K_\alpha$  as in (13), solving for  $\lambda$  yields the result.

## APPENDIX II PROOF OF THEOREM 1

To demonstrate the above let the interfering signals and the desired signal be Nakagami fading with different parameters  $m_i$  and  $m_o$  respectively. For  $m_o$  the fading parameter of the intended signal, the CCDF of the received power is:

$$F_{S_0}^c(s) = 1 - \mathbf{P}(S_0 < s) = e^{-m_o s} \sum_{k=0}^{m_o-1} \frac{(m_o s)^k}{k!}$$

with  $m_o = 1$  being the Rayleigh case. According to Lemma 1:

$$\mathbf{P}(SIR \geq \beta) = \sum_{k=0}^{m_o-1} \frac{(-\zeta)^k}{k!} \frac{d^k}{d\zeta^k} \mathcal{L}_{I_\Phi}(\zeta) \Big|_{\zeta=m_o \beta R^\alpha} \quad (59)$$

Note that  $\zeta$  now includes the fading parameter  $m_o$ . To determine the Laplace transform of the shot noise process, with  $m_i$  denoting the Nakagami parameter for all interfering transmissions the MGF of each mark is altered to be

$$E \left[ e^{-\zeta S_i |x|^{-\alpha}} \right] = \frac{1}{(1 + \zeta/m_i |x|^\alpha)^{m_i}} \quad (60)$$

and the integral in (6) can be evaluated as [44]

$$\begin{aligned} \mathcal{L}_{I_\Phi}(\zeta) &= \exp \left\{ -2\pi\lambda \int_0^\infty u \left( 1 - \frac{1}{(1 + u^\alpha/\zeta)^{m_i}} \right) du \right\} \\ &= \exp \left\{ -2\pi\lambda \int_0^\infty \frac{\sum_{k=1}^{m_i} \binom{m_i}{k} u^{k\alpha+1} (m_i/\zeta)^k}{(1 + u^\alpha m_i/\zeta)^{m_i}} du \right\} \\ &= \exp \left\{ -\lambda C_{\alpha, m_i} \left( \frac{\zeta}{m_i} \right)^{\frac{2}{\alpha}} \right\} \end{aligned} \quad (61)$$

where

$$C_{\alpha, m_i} = \frac{2\pi}{\alpha} \sum_{k=0}^{m_i-1} \binom{m_i}{k} B \left( \frac{2}{\alpha} + k; m_i - \left( \frac{2}{\alpha} + k \right) \right) \quad (62)$$

with  $B(a; b) = \frac{\Gamma(a)\Gamma(b)}{\Gamma(a+b)}$  being the beta function. According to Lemma 1, for small outage constraints  $\epsilon$ , the optimal contention density is:

$$\lambda_\epsilon = \frac{m_i^{\frac{2}{\alpha}} K_{\alpha, m_i} \epsilon}{m_o^{\frac{2}{\alpha}} C_{\alpha, m_i} \beta^{\frac{2}{\alpha}} R^2} \quad (63)$$

where  $K_{\alpha, 1} = 1$  and for  $m_o \geq 2$  it is given by

$$K_{\alpha, m_o} = \left[ 1 + \sum_{k=0}^{m_o-2} \frac{1}{(k+1)!} \prod_{l=0}^k (l - 2/\alpha) \right]^{-1}. \quad (64)$$

If  $m_o$  is set to 1 (Rayleigh fading) with  $K_{\alpha, 1} = 1$ , and  $m_i \rightarrow \infty$ , the MGF of the power fading mark on each interferer approaches  $e^{-\zeta |x|^{-\alpha}}$ . Hence,

$$\begin{aligned} \mathcal{L}_{I_\Phi}(\zeta) &= \exp \left\{ -2\pi\lambda \int_0^\infty x (1 - e^{-\zeta |x|^{-\alpha}}) dx \right\} \\ &= \exp \left\{ -2\pi\lambda \left( -\frac{1}{\alpha} \zeta^{\frac{2}{\alpha}} \Gamma(2/\alpha) \right) \right\} \\ &= \exp \left\{ -\pi\lambda \zeta^{\frac{2}{\alpha}} \Gamma(1 - 2/\alpha) \right\} \end{aligned} \quad (65)$$

indicating that

$$\lim_{m \rightarrow \infty} \frac{C_{\alpha, m}}{m^{\frac{2}{\alpha}}} = \pi \Gamma(1 - 2/\alpha). \quad (66)$$

If in addition  $m_i = \infty$  with  $C_{\alpha, \infty} = \pi \Gamma(1 - 2/\alpha)$  and  $m_o$  is allowed to approach infinity, the distribution of  $S_0$  becomes an impulse at  $S_0 = 1$ . Weber, *et al.* [14], derived bounds on the optimal contention density for path loss only (non-fading):

$$\left( \frac{\alpha - 1}{\alpha} \right) \frac{\epsilon}{\pi \beta^{\frac{2}{\alpha}} R^2} \leq \lambda_\epsilon \leq \frac{\epsilon}{\pi \beta^{\frac{2}{\alpha}} R^2}.$$

This gives

$$\left( \frac{\alpha - 1}{\alpha} \right) \frac{1}{\pi} \leq \lim_{m \rightarrow \infty} \frac{K_{\alpha, m}}{C_{\alpha, m}} \leq \frac{1}{\pi} \quad (67)$$

which for fixed  $C_{\alpha, \infty}$  determines the asymptotic orderwise increase of  $K_{\alpha, m}$ :

$$\lim_{m \rightarrow \infty} \frac{K_{\alpha, m}}{m^{\frac{2}{\alpha}}} = c_1 \quad (68)$$

for some finite, nonzero constant  $c_1$ . To fully demonstrate the orderwise behavior of  $K_{\alpha, m}$ , the bounds

$$1 \leq \frac{K_{\alpha, m}}{m^{\frac{2}{\alpha}}} \leq c_1 \quad (69)$$

hold since  $\frac{K_{\alpha, m}}{m^{\frac{2}{\alpha}}}$  is monotonically increasing but approaches the limit  $c_1$ . The monotonicity of  $\frac{K_{\alpha, m}}{m^{\frac{2}{\alpha}}}$  is shown in the next appendix.

Equation (63) is more general than (14) for which  $m_o = m_i = m$ , but while the physical significance of modeling this disparity between desired and interfering statistics is dubious<sup>1</sup>, it allows the behavior of  $K_{\alpha, m}$  and  $C_{\alpha, m}$  to be studied. It was shown in [14] that the upper bound is fairly tight which implies that in fact  $\lim_{m \rightarrow \infty} \frac{K_{\alpha, m}}{C_{\alpha, m}} \approx \frac{1}{\pi}$ . While the upper bound holds, we have numerically that the ratio  $\frac{K_{\alpha, m}}{C_{\alpha, m}}$  does in fact approach the upper bound with increasing  $m$ . Approximating closely the limit  $\frac{K_{\alpha, \infty}}{C_{\alpha, \infty}}$  as  $\frac{1}{\pi}$ , we can approximate  $c_1$  very closely as  $c_1 \approx \Gamma(1 - 2/\alpha)$ .

<sup>1</sup>For moderately dense ad hoc or sensor networks with narrowband transmission, the key interferers are the nearest ones, and it is unlikely that the propagation statistics of the interfering and desired signals would be widely different.

APPENDIX III  
PROOF OF THE MONOTONICITY OF  $\frac{K_{\alpha,m}}{m^{\frac{2}{\alpha}}}$

It is demonstrated inductively that  $\frac{K_{\alpha,m}}{m^{\frac{2}{\alpha}}}$  is monotonically increasing with increasing  $m$ . First, note that

$$\begin{aligned} K_{\alpha,m}^{-1} &= 1 + \sum_{k=0}^{m-2} \frac{1}{(k+1)!} \prod_{l=0}^k (l - 2/\alpha) \\ &= 1 - \sum_{k=0}^{m-2} \frac{\Gamma(k - \frac{2}{\alpha})}{\Gamma(k+2)\Gamma(\frac{2}{\alpha})} \\ &= K_{\alpha,m-1}^{-1} - \frac{\Gamma(m-2-\frac{2}{\alpha})}{\Gamma(m)\Gamma(\frac{2}{\alpha})} \end{aligned} \quad (70)$$

for  $\Gamma(\cdot)$  the complete gamma function. For  $m = 1$ , the ratio  $\frac{K_{\alpha,m}}{m^{\frac{2}{\alpha}}} = 1$ , while for  $m = 2$ ,

$$\frac{K_{\alpha,m}}{m^{\frac{2}{\alpha}}} = \frac{1}{2^{\frac{2}{\alpha}}(1 - \frac{2}{\alpha})} > 1.$$

To continue with the induction, we show instead that  $\frac{m^{\frac{2}{\alpha}}}{K_{\alpha,m}}$  is monotonically decreasing. Now if

$$(m+1)^{\frac{2}{\alpha}} K_{\alpha,m+1}^{-1} < m^{\frac{2}{\alpha}} K_{\alpha,m}^{-1} \quad (71)$$

suppose also that

$$\left(m^{\frac{2}{\alpha}} + \frac{2}{\alpha} m^{\frac{2}{\alpha}-1}\right) K_{\alpha,m+1}^{-1} < m^{\frac{2}{\alpha}} K_{\alpha,m}^{-1} \quad (72)$$

since  $m^{\frac{2}{\alpha}} + \frac{2}{\alpha} m^{\frac{2}{\alpha}-1} > (m+1)^{\frac{2}{\alpha}}$  for  $\alpha > 2$  with  $m^{\frac{2}{\alpha}}$  a concave function. This also implies the first condition (71) as well. Thus,

$$\begin{aligned} \frac{2}{\alpha} m^{\frac{2}{\alpha}-1} K_{\alpha,m+1}^{-1} &< m^{\frac{2}{\alpha}} \frac{\Gamma(m-1-\frac{2}{\alpha})}{\Gamma(m+1)\Gamma(\frac{2}{\alpha})} \\ K_{\alpha,m+1}^{-1} &< \frac{\alpha m \Gamma(m-1-\frac{2}{\alpha})}{2 \Gamma(m+1)\Gamma(\frac{2}{\alpha})}. \end{aligned} \quad (73)$$

To show the induction, we need

$$(m+2)^{\frac{2}{\alpha}} K_{\alpha,m+2}^{-1} < (m+1)^{\frac{2}{\alpha}} K_{\alpha,m+1}^{-1}$$

but this condition holds if

$$\begin{aligned} \left(m^{\frac{2}{\alpha}} + \frac{2}{\alpha} m^{\frac{2}{\alpha}-1} \frac{2}{\alpha} (m+1)^{\frac{2}{\alpha}-1}\right) K_{\alpha,m+2}^{-1} \\ < \left(m^{\frac{2}{\alpha}} + \frac{2}{\alpha} m^{\frac{2}{\alpha}-1}\right) K_{\alpha,m+1}^{-1}. \end{aligned} \quad (74)$$

Beginning with the desired condition (74) above, this implies

$$\begin{aligned} \frac{2}{\alpha} (m+1)^{\frac{2}{\alpha}-1} K_{\alpha,m+1}^{-1} \\ < \frac{\Gamma(m-\frac{2}{\alpha})}{\Gamma(m+2)\Gamma(\frac{2}{\alpha})} \left(m^{\frac{2}{\alpha}} + \frac{2}{\alpha} m^{\frac{2}{\alpha}-1} + \frac{2}{\alpha} (m+1)^{\frac{2}{\alpha}-1}\right) \end{aligned} \quad (75)$$

Substituting from (73), (74) holds if

$$\begin{aligned} (m+1)^{\frac{2}{\alpha}-1} \frac{m \Gamma(m-1-\frac{2}{\alpha})}{\Gamma(m+1)} \\ < \frac{\Gamma(m-\frac{2}{\alpha})}{\Gamma(m+2)} \left(m^{\frac{2}{\alpha}} + \frac{2}{\alpha} m^{\frac{2}{\alpha}-1} + \frac{2}{\alpha} (m+1)^{\frac{2}{\alpha}-1}\right) \end{aligned} \quad (76)$$

$$(m+1)^{\frac{2}{\alpha}} < m^{\frac{2}{\alpha}} + \frac{2}{\alpha} m^{\frac{2}{\alpha}-1} + \frac{2}{\alpha} (m+1)^{\frac{2}{\alpha}-1} \quad (77)$$

which is true by concavity of  $m^{\frac{2}{\alpha}}$  since the RHS is a two point linear approximation to  $(m+2)^{\frac{2}{\alpha}}$  for any  $m > 2$ .

ACKNOWLEDGEMENT

The authors thank Dr. Aamir Hasan, Dr. Sanjay Shakkottai, and Vikram Chandrasekhar for many helpful conversations.

REFERENCES

- [1] C. Rao and B. Hassibi, "Analysis of multiple-antenna wireless links at low SNR," *submitted to IEEE Trans. Inf. Theory*.
- [2] W. Choi and J. Andrews, "Spatial multiplexing in cellular MIMO-CDMA systems with linear receivers: Outage probability and capacity," *to appear IEEE Trans. Wireless Comm.*, Aug. 2004.
- [3] P. Gupta and P. R. Kumar, "The capacity of wireless networks," *IEEE Trans. on Info. Theory*, vol. 46, no. 2, pp. 388–404, Mar. 2000.
- [4] F. Xue, L.-L. Xie, and P. R. Kumar, "The transport capacity of wireless networks over fading channels," *IEEE Trans. on Info. Theory*, vol. 51, no. 3, pp. 834–847, Mar. 2005.
- [5] L.-L. Xie and P. R. Kumar, "On the path-loss attenuation regime for positive cost and linear scaling of transport capacity in wireless networks," *IEEE Trans. on Info. Theory*, vol. 52, no. 6, pp. 2313–2328, June 2006.
- [6] L. Xie and P. R. Kumar, "A network information theory for wireless communication: scaling laws and optimal operation," *IEEE Trans. on Info. Theory*, vol. 50, no. 5, pp. 748–767, May 2004.
- [7] O. Leveque and I. E. Telatar, "Information-theoretic upper bounds on the capacity of large extended ad hoc wireless networks," *IEEE Trans. on Info. Theory*, vol. 51, no. 3, pp. 858–865, Mar. 2005.
- [8] M. Grossglauser and D. Tse, "Mobility increases the capacity of ad-hoc wireless networks," *IEEE/ACM Trans. on Networking*, vol. 10, pp. 477–486, Aug. 2002.
- [9] M. J. Neely and E. Modiano, "Capacity and delay tradeoffs for ad-hoc mobile networks," *IEEE Trans. on Info. Theory*, vol. 51.
- [10] P. Gupta and P. R. Kumar, "Critical power for asymptotic connectivity in wireless networks," *IEEE Conference on Decision and Control*, 1998.
- [11] S. Toumpis and A. J. Goldsmith, "Capacity regions for wireless ad hoc networks," *IEEE Trans. on Wireless Communications*, vol. 2, no. 4, pp. 736–748, July 2003.
- [12] S. Ye and R. S. Blum, "On the rate region for wireless MIMO ad hoc networks," *VTC-Fall 2004 Los Angeles, USA*, vol. 3.
- [13] R. Gowaikar, B. Hochwald, and B. Hassibi, "Communication over a wireless network with random connections," *IEEE Trans. on Info. Theory*, vol. 52, no. 7, pp. 2857–2871, July 2006.
- [14] S. Weber, X. Yang, J. G. Andrews, and G. de Veciana, "Transmission capacity of wireless ad hoc networks with outage constraints," *IEEE Trans. on Info. Theory*, vol. 51, no. 12, pp. 4091–4102, Dec. 2005.
- [15] F. Baccelli, B. Blaszczyzyn, and P. Muhlethaler, "An ALOHA protocol for multihop mobile wireless networks," *IEEE Trans. on Info. Theory*, vol. 52, no. 2, pp. 421–436, Feb. 2006.
- [16] J. Silvester and L. Kleinrock, "On the capacity of multihop slotted ALOHA networks with regular structure," *IEEE Trans. on Communications*, vol. 31, no. 8, pp. 974–982, Aug. 1983.
- [17] L. Kleinrock and J. Silvester, "Spatial reuse in packet radio networks," *Proceedings of the IEEE*, vol. 75, no. 1, pp. 156–167, Jan. 1987.
- [18] C. Chan and S. V. Hanly, "Calculating the outage probability in a CDMA network with spatial poisson traffic," *IEEE Trans. on Veh. Technology*, vol. 50, no. 1, pp. 183–204, Jan. 2001.
- [19] M. Haenggi, "Analysis and design of diversity schemes for ad hoc wireless networks," *IEEE Journal on Sel. Areas in Communications*, vol. 23, no. 1, pp. 19–27, Jan. 2005.
- [20] X. Liu and M. Haenggi, "Throughput analysis of fading sensor networks with regular and random topologies," *EURASIP J. of Wireless Comm. and Net.*, vol. 4, pp. 554–564, Aug. 2005.
- [21] R. K. Ganti and M. Haenggi, "Regularity, interference, and capacity of large ad hoc networks," *Proc., IEEE Asilomar*, Oct. 2006.
- [22] S. Srinivasa and M. Haenggi, "Simplified analysis and design of MIMO ad hoc networks," *Proc., IEEE Globecom*, Nov. 2006.
- [23] I. E. Telatar, "Capacity of multi-antenna Gaussian channels," *Eur. Trans. Telecomm. ETT*, vol. 10, no. 6, pp. 585–596, Nov. 1999.

- [24] A. J. Goldsmith, S. A. Jafar, N. Jindal, and S. Vishwanath, "Capacity limits of MIMO channels," *IEEE Journal on Sel. Areas in Communications*, vol. 21, no. 5, pp. 684–702, June 2003.
- [25] A. Shah and A. M. Haimovich, "Performance analysis of maximal ratio combining and comparison with optimum combining for mobile radio communications with co-channel interference," *IEEE Trans. on Veh. Technology*, vol. 49, no. 4, pp. 1454–1463, July 2000.
- [26] M. Kang and M.-S. Alouini, "Largest eigenvalue of complex Wishart matrices and performance analysis of MIMO MRC systems," *IEEE Journal on Sel. Areas in Communications*, vol. 21, no. 3, pp. 418–426, Apr. 2003.
- [27] —, "A comparative study on the performance of MIMO MRC systems with and without cochannel interference," *IEEE Trans. on Communications*, vol. 52, no. 8, pp. 1417–1425, Aug. 2004.
- [28] R. S. Blum, "MIMO capacity with interference," *IEEE Journal on Sel. Areas in Communications*, vol. 21, no. 5, pp. 793–801, June 2003.
- [29] B. Chen and M. J. Gans, "MIMO communications in ad hoc networks," *IEEE Trans. on Signal Processing*, vol. 54, no. 7, pp. 2773–2783, July 2006.
- [30] X. Yu, R. de Moraes, H. Sadjadpour, and J. J. Garcia-Luna-Aceves, "Capacity of MIMO mobile wireless ad hoc networks," *Wirelesscomm, Maui, HI.*, vol. 2, pp. 1053–1058, June 2005.
- [31] D. Stoyan, W. Kendall, and J. Mecke, *Stochastic Geometry and Its Applications*, 2nd ed. John Wiley and Sons, 1996.
- [32] J. F. C. Kingman, *Poisson Processes*. USA: Oxford University Press, 1993.
- [33] G. L. Stuber, *Principles of Mobile Communication*, 2nd ed. Boston: Kluwer Academic Publishers, 2001.
- [34] R. Ramanathan, J. Redi, C. Santivanez, D. Wiggins, and S. Polit, "Ad hoc networking with directional antennas: a complete solution," *IEEE Journal on Sel. Areas in Communications*, vol. 23, no. 3, pp. 496–506, Mar. 2005.
- [35] R. R. Choudhury, X. Yang, R. Ramanathan, and N. H. Vaidya, "On designing MAC protocols for wireless networks using directional antennas," *IEEE Trans. Mobile Comp.*, vol. 5, no. 5, pp. 477–491, May 2006.
- [36] C. A. Balanis, *Antenna Theory: Analysis and Design*. New York: Harper and Row Publishers, 1982.
- [37] T. K. Y. Lo, "Maximum ratio transmission," *IEEE Trans. on Communications*, vol. 47, no. 10, pp. 1458–1461, Oct. 1999.
- [38] C. G. Khatri, "Distribution of the largest or the smallest characteristic root under null hypothesis concerning complex multivariate normal populations," *Ann. Math. Stat.*, vol. 35, pp. 1807–1810, Dec. 1964.
- [39] R. A. Horn and C. R. Johnson, *Matrix Analysis*. Cambridge: Cambridge University Press, 1985.
- [40] E. G. Larsson and P. Stoica, *Space-Time Block Coding for Wireless Communications*. Cambridge: Cambridge University Press, 2003.
- [41] S. M. Alamouti, "A simple transmit diversity technique for wireless communications," *IEEE Journal on Sel. Areas in Communications*, vol. 16, no. 8, pp. 1451–1458, Oct. 1998.
- [42] A. Paulraj, R. Nabar, and D. Gore, *Introduction to Space-Time Wireless Communications*. Cambridge: Cambridge University Press, 2003.
- [43] W. Choi, N. Himayat, S. Talwar, and M. Ho, "The effect of co-channel interference on spatial diversity techniques," *submitted to IEEE WCNC 2007*.
- [44] I. S. Gradshteyn and I. M. Ryzhik, *Table of Integrals, Series, and Products*, 6th ed. London: Academic Press, 2000.